

DOI: 10.24850/j-tyca-2024-03-04

Articles

Comparison of a single and two-armed hydraulic ram in parallel with vertical-radial supply pipe

Comparación de uno y dos arietes hidráulicos en paralelo con suministro vertical-radial

Efraín del Risco Moreno¹, ORCID: <https://orcid.org/0000-0003-2563-8265>

Rubén D. Muelas-Hurtado², ORCID: <https://orcid.org/0000-0002-2877-6682>

Esnel A. Acosta P.³, ORCID: <https://orcid.org/0009-0008-2655-5756>

¹Universidad del Valle, Cali, Colombia, efrain.del@correounivalle.edu.co

²Universidad del Valle, Cali, Colombia; Instituto de Ciencias Físicas, Cuernavaca, Morelos, Mexico, ruben.muelas@correounivalle.edu.co

³Universidad del Valle, Cali, Colombia, esnel.acosta@correounivalle.edu.co

Corresponding author: Rubén D. Muelas-Hurtado, ruben.muelas@correounivalle.edu.co



Abstract

The behavior of a single and two hydraulic rams simultaneously operating in parallel, with and without downpipe (addition to the delivery conduction), and vertical-horizontal downward supply is analyzed and compared through experimental data. This study was performed using a configurable hydraulic circuit with the capacity to operate with constant delivery head and variable supply head for both single and two-armed ram configuration. The flow rates delivered and pumped by the hydraulic rams were measured for each supply head, and the pressure in the main pipeline —near each ram— in the air chamber, and the delivery pipe were recorded. A comparison of the performance for a single and two hydraulic rams in parallel operation is reported by first time. For this, flow rates, pressure at different point on the hydraulic circuit, water hammer frequency, and efficiency of both configurations were measured and compared. The results show that two rams operating in parallel present a similar behavior to the well-known radial pumps. As some studies reported, the frequency of the water hammer and the pumped flow rates increase with delivery head. However, the most significant result mentioned in this work is the increase of the water hammer frequency that result in an increase of the pumped flow rate because of the downpipe attached to the hydraulic circuit. This research contributes to the development of multiple hydraulic rams with standard supply, with parallel or individual discharges, to pump more water than current designs used so far.

Keywords: Hydraulic rams, pumps, water hammer, unsteady flow, pumping system.

Resumen

Mediante datos experimentales se analiza y compara el comportamiento de uno y dos arietes hidráulicos en paralelo con y sin bajante (adición a la conducción de entrega), y suministro descendente vertical-radial. El estudio se hizo en un circuito hidráulico configurable para que esos dispositivos operen de una u otra forma a altura de entrega constante y altura de suministro variable. Con cada altura de suministro se midieron los caudales suministrados y bombeados por los arietes hidráulicos, y la presión en la tubería de impulsión —cerca de cada ariete— en la cámara de aire y en la tubería de entrega. Esta información permitió comparar por primera vez el desempeño de arietes hidráulicos funcionando solos o en paralelo mediante el análisis de caudales, presiones, frecuencia del golpe y eficiencia de los dispositivos. Como las bombas radiales, los resultados indican que dos arietes hidráulicos en paralelo entregan más que uno, pero menos que la suma del caudal bombeado por cada uno con descarga independiente. En el rango de alturas de suministro ensayado, la frecuencia del golpe de ariete y el caudal bombeado crecen con la altura de suministro, como se reporta en otros estudios. No obstante, el resultado más destacado es el efecto del bajante, porque incrementa varias veces el caudal bombeado al aumentar la frecuencia del golpe de ariete. Esta investigación impulsa el desarrollo de un sistema de múltiples arietes hidráulicos con suministro común, y descargas en paralelo o individuales para bombear más que con los diseños actuales.

Palabras clave: arietes hidráulicos, bombas, golpe de ariete, flujo inestable, sistema de bombeo.

Received: 02/08/2021

Accepted: 26/08/2022

Published Online: 28/11/2022

Introduction

For inhabitants of isolated rural areas with water sources located at lower levels, raising this liquid is an important task that influences their different daily activities and their quality of life (IDRC-MR102eR, 1986). While for developed countries this difficulty was overcome by using pumping systems driven by electric or internal combustion machines, for developing countries this is still a current problem that drastically affects the water supply (DTU, 1996). The irresponsible management of natural resources, e.g., water, has led to a significant deterioration of the environment. Some examples are the negative impact to the environment due to large (Rosenberg, Bodaly, & Usher, 1995) and small hydroelectric power plants (Steinmetz & Sundqvist, 2014) that cause the extinction of some animal and vegetable species (Cahill *et al.*, 2013).

Likewise, the greenhouse gases because of products of combustion have contributed to the global warming of the planet (El Zein & Chehayeb, 2015; Kweku *et al.*, 2018). Hence, the use of energy from renewable sources is one of the most pressing goals in the modern industry (Manzini, Islas, & Martínez, 2001; Alrikabi, 2014). In this sense, hydraulic ram is becoming important as an alternative water pumping system for water

supply and as a source of clean energy conversion, since it takes advantages of the Earth's gravitational potential, its initial and maintenance costs are low, and more importantly, it does not contaminate the environment s (Young, 1998).

The hydraulic ram is a simple device that works intermittently due to the water hammer generated when its delivery valve closes. However, only a small part of the supplied flow is delivered (Rennie & Bunt, 1990). The study of this mechanical system is complex, even when the only moving parts are the impulse and delivery valve, because it operates with an unsteady flow.

Originally, this fluid machine was experimentally investigated and later an attempt to predict its behavior was analytically proposed. This analytical approach was unsuccessful because certain constants could not be determined through experiments. Therefore, this led to the use of the rational method that combines theory and experimentation.

Since the invention of the hydraulic ram (1776) until the third decade of the 20th century, the effort to study this device was insufficient due to the neglect of some effects, such as, energy losses due to friction and turbulence, the length of the drive valve stroke, the elasticity of water and pipe material, etcetera (Krol, 1947).

In a rational study (Lansford & Dugan, 1941) developed a theoretical model that predicts results accordant with experimental data but differs for hydraulic rams with smaller diameters. Similarly, with an analytical model whose constants were experimentally determined, Krol (1947) incorporated the effects of turbulence and the weight of the

impulsion valve disc, achieving a good approximation between the values of the measured and calculated variables.

Subsequently, a hydraulic ram was analyzed as a function of time and the ration between impulse and delivery load and without considering the effects of short-term pressure fluctuations (Iversen, 1975). Thus, more thoroughly coherence between the calculated and measured variables, as well as the efficiency rate for larger height ratios.

With a simple analytical model, a successful prediction of the efficiency, the pumped flow rate, and the period of a pumping cycle of a hydraulic ram was achieved (Schiller & Kahangire, 1984). In a similar way, by using the method of characteristics, a discrete technique was tested in hydraulic transient flows (Glover, 1994), and the unsteady flow equations in a hydraulic ram were solved, contributing to a better understanding of its operation and providing a new work tool in the conceptual design stage. With the same solution technique (Najm & Azoury, 1999) studied the possible states of a hydraulic ram, including the air chamber and the delivery pipe. This technique was also used to solve unsteady flow equations system when modeling each element of the hydraulic ram (Filipan, Virag, & Bergant, 2003) using supply and storage tanks as boundary conditions.

After a while (De-Carvalho, Diniz, & Neves, 2011) presents a model to predict the dynamic behavior of a hydraulic ram following the numerical approach to provide a design tool with scientific bases. The predictions of all these studies were successfully compared with experimental results. More recently, the influence of the length of the deliver pipe and the height of the storage tank on the performance of the hydraulic ram was

studied using the experimental method (Jafri & Sanusi, 2019). Other parameters, such as the length of the stroke of the delivery valve, for a commercial ram, was investigated and results showed that there is an optimal value for both, the length of the stroke and delivery pipe, which maximizes the pumped flow rate (Arapa Quispe, 2016).

The influence of the stroke of the impulsion valve on the pumped flow rate was analyzed using the rational method (Krol, 1947; Januddi *et al.*, 2018) demonstrating that there is a value of this parameter that also maximizes the pumped flow rate. The closing of the impulse valve is a rapid process that occurs in the final stretch (20 %) of the stroke. To observe this behavior, a high-speed photography (Viccione, Immediata, Cava, & Piantedosi, 2018) was used to correlate the closing with the increase in the pressure associated to water hammer.

To provide a better understanding of the starting condition of the impulse valve (Sobieski, Lipin, & Grygo, 2020) used the experimental method to define the filling condition of the ram during its automatic start. Another study reports that under certain characteristics of the impulse valve, the frequency of the water hammer is ten times greater than that of the delivery valve (Sobieski, Grygo, & Lipiński, 2016). The forces of the delivery valve during the flow acceleration were also studied to determine the speed at the end of the stage. In the same work, a numerical analysis is presented and the pressure and forces acting under those conditions are estimated (Sobieski & Grygo, 2019).

Using a modified impulse valve the stroke of this device was adjusted to increase the pumped flow rate and the delivery height (Credo & Metra, 2020). Another key component in the operation of the air

chamber is the reset valve. It was determined that a diameter of 1 mm of the orifice on this element improves the behavior of the hydraulic ram (Sucipta & Suarda, 2019). Likewise, the effect of the tilting angle of the delivery valve on the operation of a hydraulic ram has been experimentally studied (Suarda, Kusuma, Sucipta, & Ghurri, 2020) demonstrating that an angle of 60 degrees optimizes the performance of this device during the pumping stage.

In other researches, the geometry of delivery valves increase the efficiency of the hydraulic circuit, especially when a ball valve is used (Suarda *et al.*, 2020). In addition, Kimaro and Salaam (2018), and Ngolle and Hong (2019) reported the influence of the volume of the air chamber on the pumped flow rate. However, in both studies results are divergent because the first reports an influence of the pumped flow rate due to the air chamber volume, as found experimentally by Krol (1947), while the second states that the volume does not affect the pumped flow.

In the same way, springs have been added to the impulse and deliver valve and to the air chambers to demonstrate the influence on the pumped flow rate (Rajaonison & Rakotondramiarana, 2020). A comparison between theory and experiments shows that there is a good agreement only for strokes less or equal than a length of 8 mm.

Based on the literature review presented, hydraulic rams has only been operated using independent supply and delivery pipes. Only one manuscript reports a parallel ram connection (Pramono, Suharno, & Widodo, 2018) where the total pumped flow rate less than 3 l/min is obtained. There are no details on the experiment or pressure measurements. Moreover, in the literature, the configuration of the

hydraulic circuit consists of a tilted supply pipeline (conventional) with horizontal connection and lateral water supply. To date, there is no information of other circuit configurations where the supply pipe is vertical radial as presented in this study.

This manuscript reports the increase in the pumped flow rate when two rams share the same supply and delivery pipes. Hence, the name of parallel rams.

To compare the flow rate pumped by a single and two-armed hydraulic rams operating in parallel, a configurable hydraulic circuit was designed and fabricated to be operated in both configurations. For both, the following variables are measured: 1) the supplied and pumped flow rates, 2) the instantaneous pressure in different and of-interest-positions in the hydraulic circuit, and 3) the water hammer frequency obtained from the pressure signals. The analysis presented allow to identify the behavior of these devices under the proposed conditions aimed to design more compact and efficient hydraulic circuits that those reported to date.

Single hydraulic ram-conventional configuration

A hydraulic ram is an autonomous pump device that is driven by the potential energy difference and establishes an oscillating flow in its delivery pipe connected to supply tank when the delivery valve is closed (Figure 1I). It also has a delivery valve that allows water to flow from the supply pipeline to the air chamber (Figure 1II), which dampens the vibrations induced by water hammer and maintains the water pressure in the delivery pipe.

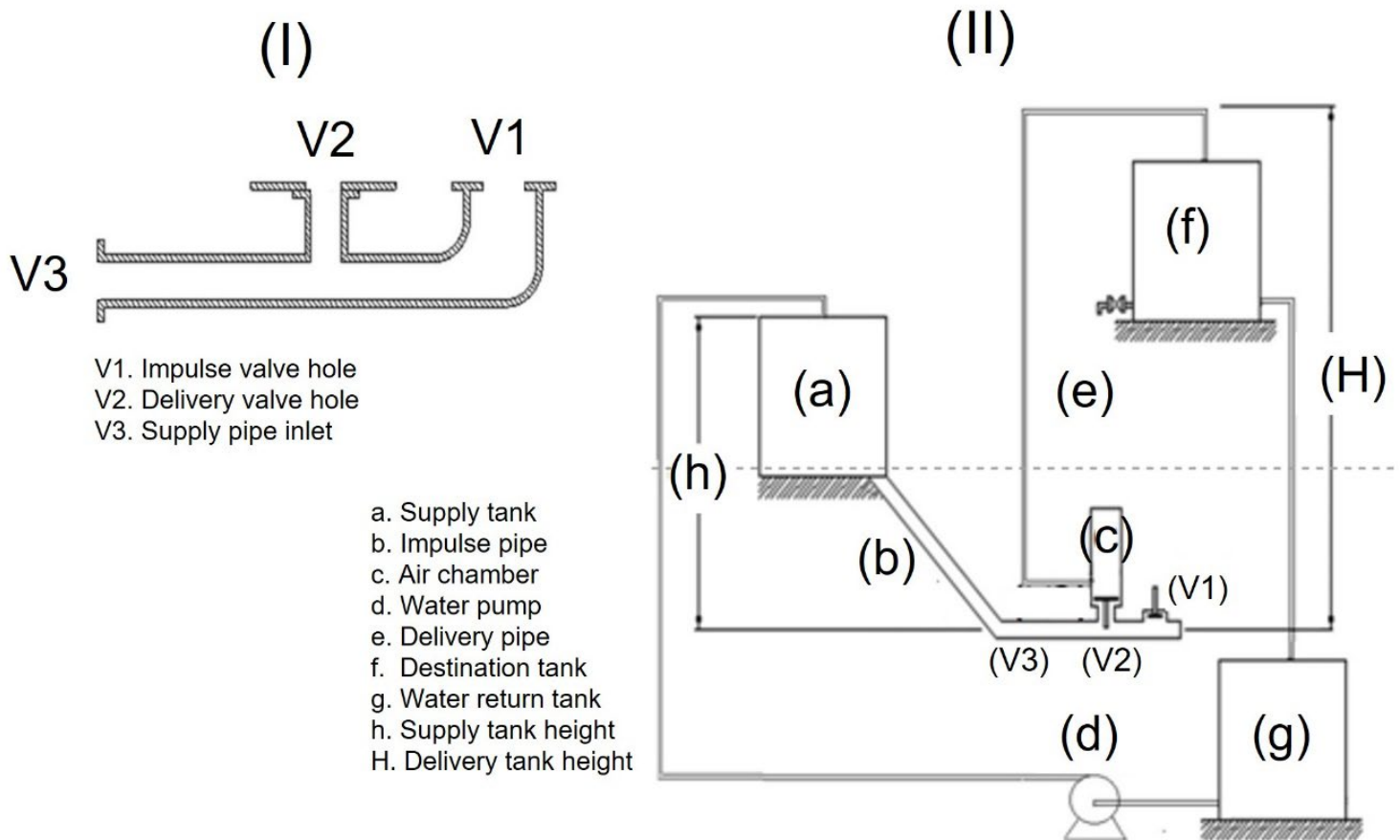


Figure 1. (I) Hydraulic ram body y (II) hydraulic circuit.

The pumping capacity of the hydraulic rams increases when water is individually supplied to each ram connected to the circuit and the discharge, that is the final section of the delivery pipeline, share a common pipeline (Watt, 1974; Silver, 1977), that is to say, they are connected in parallel.

The complete stages of a hydraulic ram during an operating cycle according to Landsford and Dugan (1941), and Krol (1947) are divided in

seven steps, however, Tacke (1988) declares they are six. There is no report about the operation of hydraulic rams with parallel discharge.

To illustrate the operation of a single hydraulic ram duty cycle, a summary of Krol's analysis suggests:

Stage 1. Closed impulse valve-closed delivery valve: Water returns to the impulse pipe from the air chamber because the pressure in the impulse pipe decreases.

Stage 2. Open impulse valve – closed delivery valve: Water in the delivery pipe is accelerated until the drag force starts the closure of the impulse valve.

Stage 3. Closing of the impulse valve – closed delivery valve: Drag force closes the impulse valve and the pressure in the impulse pipeline exceeds the hydrostatic pressure imposed by the supply tank.

Stage 4. Opening of the delivery valve-closed impulse valve: The abrupt delay of the pressure wave in the impulse pipe opens the delivery pipe.

Stage 5. Open delivery pipe-close impulse valve: There is an intermittent flow from the impulse pipe to the air chamber, with gradual closing of the delivery valve until it completely closes. Part of the driving energy is converted into deformation energy of the pipe and water compression.

Stage 6. Closed delivery valve – closed impulse valve: The initial hydrostatic pressure returns to the impulse valve and the flow inside has a negative velocity.

Stage 7. Opening of the impulse valve-closed delivery valve: There is no drag force at the end of the previous cycle and the impulse valve opens and a new cycle begins.

When the complete operating cycle of a hydraulic ram is considered, the equations that describe its behavior becomes complex. Some authors, simplify these cycles into three (Iversen, 1974) or four (Tacke, 1988) stages. This simplification assumes that the short duration stages are negligible or assimilated to the immediately preceding one.

Theory

The analysis of the fluid motion in a hydraulic ram is non-linear due to the turbulence and the intermittency of the flow caused by the opening and closing of the impulsation valve. The flow in the delivery pipe can be studied with: a) Newton's second law ((Lansford & Dugan, 1941); b) a differential equation for unsteady flow (Iversen, 1975), or c) the unsteady flow equations in a pipeline (Tacke, 1988). Any of these alternatives requires the constants of the different elements that compose the experimental installation: pipes, accessories, and especially those associated with the turbulence and impulse valve. These constants are specific to each experimental setup; thus, the prediction of the mathematical models only describe the operation of the hydraulic ram with independents supply and delivery pipes.

There are also numerical solutions of the unsteady flow in a hydraulic ram (Glover, 1994; Filipan *et al.*, 2003; De-Carvalho *et al.*,

2011), obtained by modeling each of its elements and solving the resulting equations with the method of characteristics.

In this study experimental and analytical results (using the Tacke (1988) calculation) are compared using the relationship for a simplified operation cycle of: acceleration, retardation (pumping) and return of flow, as illustrated in Figure 2. Each stage of the reduced duty cycle of a hydraulic ram is obtained by joining the one with long period to the next with a shorter period and it is analyzed in terms of the flow velocity (u) in the delivery pipe and time (t). For this, the differential equations of continuity and motion of the unsteady flow (Ghidaoui, Zhao, McInnis, & Axworthy, 2005) in a pipe with a circular cross section:

$$\frac{1}{c^2} \frac{\partial h}{\partial t} + \frac{u}{c^2} \frac{\partial h}{\partial x} + \frac{u}{c^2} \sin \beta + \frac{1}{g} \frac{\partial u}{\partial x} = 0 \quad (1)$$

$$\frac{\partial u}{\partial t} + u \frac{\partial u}{\partial x} + g \frac{\partial h}{\partial x} + f \frac{u|u|}{2D} = 0 \quad (2)$$

where:

$$\frac{1}{c^2} = \left[\frac{\rho}{K} + \frac{\rho D}{E e} \phi \right]^{-1} \quad (3)$$

From the previous relations, the characteristic equation of this type of motion is:

$$\frac{\partial x}{\partial t} = u \pm c \quad (4)$$

$$\frac{\partial h}{\partial t} = \mp \frac{c}{g} \frac{du}{dt} \mp \frac{c}{g} f \frac{u|u|}{2D} - u \sin \beta \quad (5)$$

Where c is the sound speed in the water, and β the tilting angle of the pipeline.

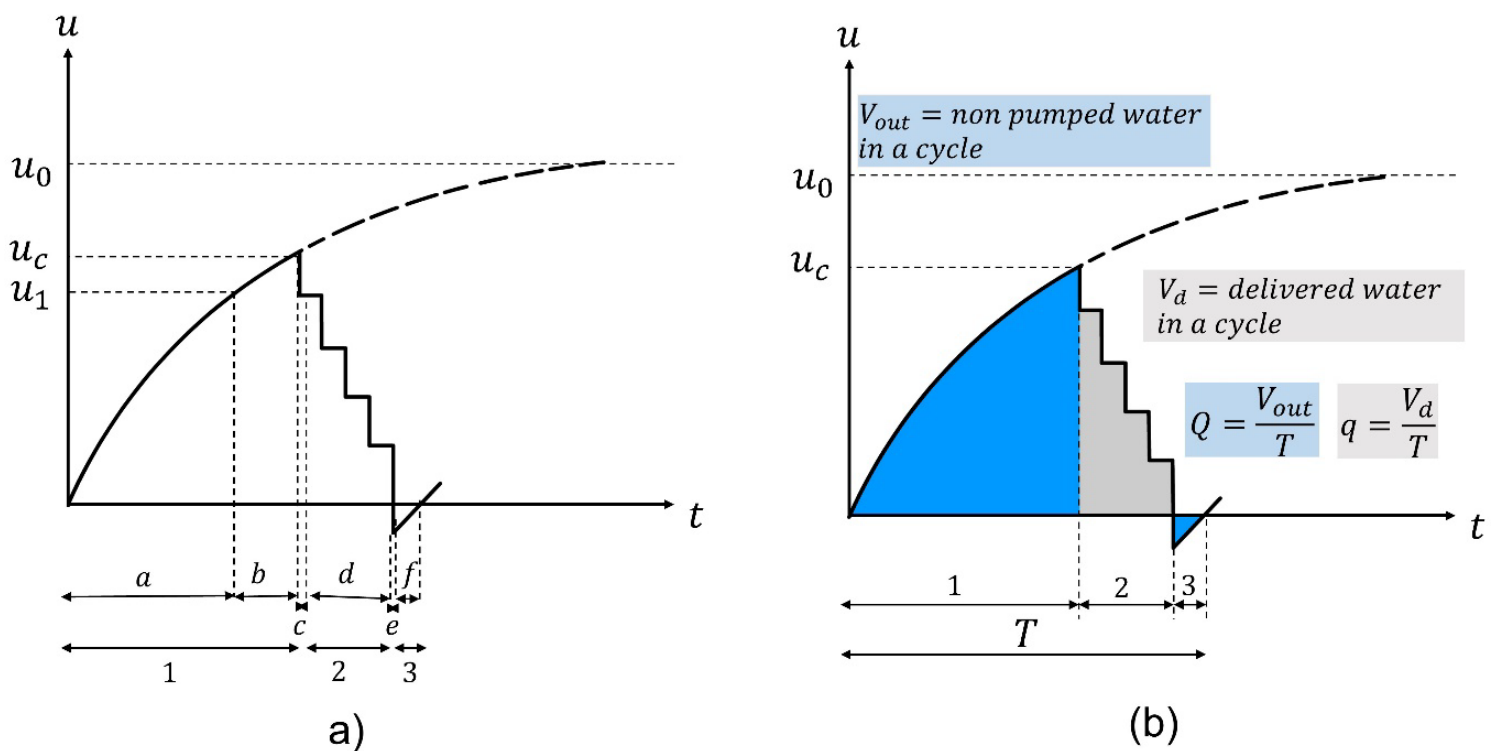


Figure 2. Schematic drawing of the ram cycles proposed by Tacke (1998) for single ram with: (a) complete cycle (b) simplified cycle.

Then the equations are simplified by an order-of-magnitude analysis with experimental data for acceleration and retardation. Thus, when the impulse valve closes, the change in the head Δh is associated with the variation of the velocity Δu of the flow in the lower end of the impulse pipe by means of the equation:

$$\Delta h = \mp \frac{c}{g} \Delta u \quad (6)$$

The \mp stands for the sudden changes in the magnitude of the pressure head in the ram or in the supply tank. The estimation of the period and flow using the three stages of the reduced cycle, according to Tacke (1988), is described as follows:

Period of acceleration (T_a)

The flow is accelerated in the impulse valve and the drag force induces the closing of the impulse valve. The flow is studied with the theory of the rigid column of water and time scale of changes in velocity of the flow (T_a) much larger than the time scale of the pressure wave velocity c ($T_a \gg \frac{2L_s}{c}$). The duration of the period (T_a) and the volume of wasted water (V_a) by the impulse valve are estimated with the following equations:

$$T_a = \frac{L_s}{u_0} \ln \left(\frac{u_0 + u_c}{u_0 - u_c} \right), u_0 = \sqrt{\frac{2gH_s}{\xi}} \quad (7)$$

$$V_a = \frac{\pi D^4}{4} \frac{2L_s}{\xi} \ln \left[\cosh \left(\frac{u_0 \xi}{2L_s} \right) \right] \quad (8)$$

where:

$$\xi = \xi_{out} + \xi_{vlv} + \xi_{in} + \xi_{fr} ; \xi_{fr} = \frac{f L_s}{D}$$

L_s is the length of the impulse pipe, u_0 the asymptotic flow velocity in the pipe when $t \rightarrow \infty$, u_c flow velocity when the impulse valve is closed, and ξ is the total coefficient of friction.

Retardation period (T_d)

The closing of the impulse valve ($t = T_a$) produces a water hammer (pressure wave) that at the speed of sound (c) propagates in both directions. For the analysis, the rapidly variable flow pressure wave is considered, neglecting primary and secondary losses, as they are much lower than the pressure from the water hammer. With Equation (5) the changes of pressure due to the supply height (Δh) are associated with the variation of speed (Δu) in the ram and the supply tank.

The variation in this stage of the operating cycle is described as follows: the closure of the delivery valve stops the flow behind it and $\Delta u = -u_c$, u_c is the valve closure speed and the pressure in the ram increases

by $\Delta h = -\frac{c}{g}\Delta u = -\frac{c}{g}(-u_c) = \frac{c}{g}u_c$. The pressure wave opens the delivery valve as it propagates from the ram to the supply tank and water flows into the air chamber at velocity $u_{1+} = u_c + \Delta u = u_c - \frac{g}{c}h_d$, because behind the pressure wavefront the water reduces its speed in proportion to $\Delta h = h_d$, and from Equation (5) in the ram $\Delta u = -\frac{g}{c}\Delta h = -\frac{g}{c}h_d$.

When the pressure waves arrives at the supply tank ($t = T_a + \frac{L_s}{c}$), the height of the water in the supply tank (H_s) does change and $\Delta h = -h_d$, therefore $\Delta u = -\frac{g}{c}h_d$ and a negative pressure wave returns to the ram with velocity $u_{1-} = u_{1+} + \Delta u = u_c - 2\frac{g}{c}h_d$.

When the pressure wave reaches the ram again ($t = T_a + \frac{2L_s}{c}$), $\Delta h = h_d$ and $\Delta u = -\frac{g}{c}h_d$, and a new positive pressure wave propagates from the ram to the supply tank with velocity $u_{2+} = u_{1-} + \Delta u = u_c - 3\frac{g}{c}h_d$.

At the instant $t = T_a + \frac{3L_s}{c}$ again the positive pressure wave reaches the supply tank and is reflected from it to the ram as a negative wave with water velocity $u_{2-} = u_{2+} - \frac{g}{c}h_d = u_c - 4\frac{g}{c}h_d$. Thus, at any time t the retardation period will be in the range $T_a + (i-1)\frac{2L_s}{c} < t < T_a + i\frac{2L_s}{c}$ and the speed of the i -th variation of pressure will be:

$$u_i = u_c - (2i - 1)\Delta u \quad (9)$$

If $i = N$, number of pressure variations during which water flows into the air chamber during retardation, then $u_N > 0$ and Equation (9) results

in $u_c - (2N - 1) \Delta u > 0$, or $u_c + \Delta u > 2N \Delta u$, with $N < \frac{u_c + \Delta u}{2 \Delta u}$; $\Delta u = \frac{c}{g} h_d$. That is, N is the largest integer such that $N < \frac{u_c + \Delta u}{2 \Delta u}$. The water then flows into the air chamber with decreasing velocity steps ending when the delivery valve closes. At that instant, the pressure wave in the ram can be:

a) **Negative**, the delivery valve opens, and the water moves away from the ram to the supply tank with the return velocity of the water from the air chamber to the impulse pipe given by

$$u_r = u_c - 2N \Delta u \quad (10)$$

b) **Positive**, the pressure wave in the ram does not have the necessary energy to generate a new pressure wave with a height equal to the delivery (h_d) and goes to the supply tank to return to the ram in $2L_s / c$ seconds later and open the impulse valve with speed:

$$u_r = 2N \Delta u - u_c \quad (11)$$

Thus, according to Tacke (1988), the equations to estimate the retarding period (T_d) and the volume of water transferred to the air chamber in this period (V_d), respectively, are:

$$T_d = N \frac{2L_s}{c} \quad (12)$$

and:

$$V_d = \frac{\pi D^2}{4} \frac{2L_s}{c} \sum_{i=1}^N u_i \quad (13)$$

where N , number of pressure changes and u_i , speed of water in the i^{th} pressure variation, $u_i = u_c - (2i - 1)\Delta u$; N , is the largest integer such that $N < \frac{u_c + \Delta u}{2\Delta u}$, where $\Delta u = \frac{c}{g} h_d$, with h_d , the delivery height.

Return period (T_r)

The closing of the delivery valve (or $2L_s/c$ seconds later) produce negative velocity in the entire impulse pipe (water goes from the ram to the supply tank). Because the delivery valve is closed ($u=$ in the ram) there is negative pressure in the body of the ram, the impulse valve opens, and the water accelerates because of the supply height H_s . The period ends when the impulse delivery valve opens and its duration T_r , and the return volume V_r , respectively, according to Tacke (1988) can be calculated with the relations:

$$T_r = \frac{u_r L_s}{g H_s} \quad (14)$$

$$V_r = -\frac{\pi D^2}{4} \frac{u_r L_s}{2g H_s} \quad (15)$$

Where case a) $u_r = u_c - 2N\Delta u$, or case b) $u_r = 2N - \Delta u - u_c$. For the case b):

$$T_r = -\frac{u_r L_s}{g H_s} + \frac{2}{L_s}, V_r = \frac{\pi D^2}{4} T_d (u_c - N\Delta u) \quad (16)$$

Finally, the delivered or pumped (q) and wasted (Q) flow rates are obtained from:

$$q = \frac{1}{T} V_d = \frac{\pi D^2}{4} \frac{T_d}{T} (u_c - N\Delta u) \quad (17)$$

$$Q = \frac{V_{out}}{T} = \frac{1}{T} (V_a + V_r) = \frac{1}{T} \frac{\pi D^2}{4} \left[\frac{2L_s}{\xi} \ln \left(\cosh \left(\frac{u_0 \xi}{2L_s} T_a \right) \right) - \frac{u_r^2 L_s}{2g H_s} \right] \quad (18)$$

$$\text{Where } T = T_a + T_d + T_r$$

Therefore, during an operating cycle of the hydraulic ram, the total flow rate (Q_t), estimated using the Tacke (1988) model is:

$$Q_t = Q + q \quad (19)$$

System performance (η)

The efficiency η of the hydraulic ram is the output power Π_{output} to input power Π_{input} ratio. This is

$$\eta = \frac{\Pi_{salida}}{\Pi_{entrada}} = \frac{\rho g H q}{\rho g h Q_t} = \frac{H q}{h Q_t} \quad (20)$$

Installation and experimental setup for hydraulic rams operating in parallel with vertical-radial downward supply, with and without return pipe

The hydraulic ram (referred to as hydram) used in this study has a drive valve built from a commercial foot-valve, with internal and external parts and female-male assembly (Figure 3). The female socket is coupled to the impulse pipe and the male socket, in the acceleration stage, discharge water to the outside through a conical grating. To convert this valve into an impulse valve, an opening and closing systems was added using a screw, a spring, and several nuts. This system compresses a spring that is in permanent contact with the commercial stem disc, which moves back and forth inside the valve. The compressed spring length was 0.1 m, with a compression range of 0.01m with steps of 0.002 m. Preliminary tests were carried out to calibrate the valve. For a spring length of 0.00875 the highest pumped flow is achieved when the impulsions valve is connected

to the hydraulic circuit with the maximum delivery height that allows a depth of 1 m of the supply tank.

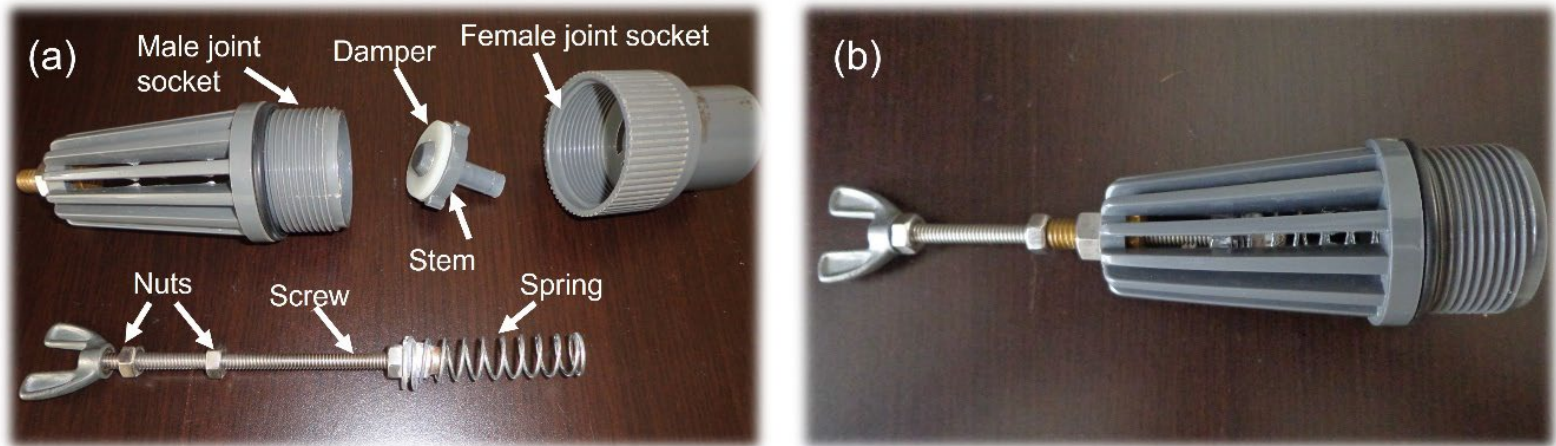


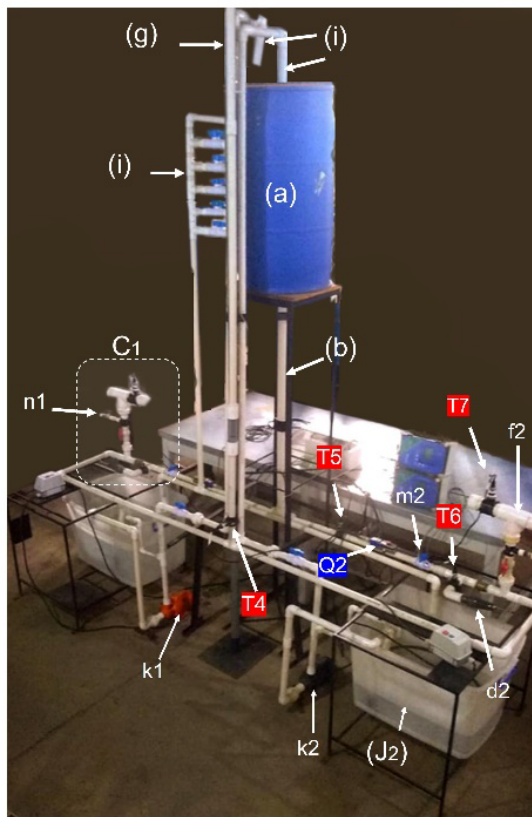
Figure 3. Impulse valve with the open/close system fabricated from a commercial foot valve. (a) Components, and (b) assembly of the valve.

Other elements of the experimental setup are: (a) delivery valve, in this study a commercial check valve of 0.0254 m in diameter was used to allow the water flow from the impulse pipe to the air chamber, and (b) horizontal air chamber built from a PVC tube of 0.0254 m in diameter and 0.2 cm of length. A general view of the experimental setup is shown in Figure 4. For the water flow, the hydraulic circuit has three sections made of PVC:

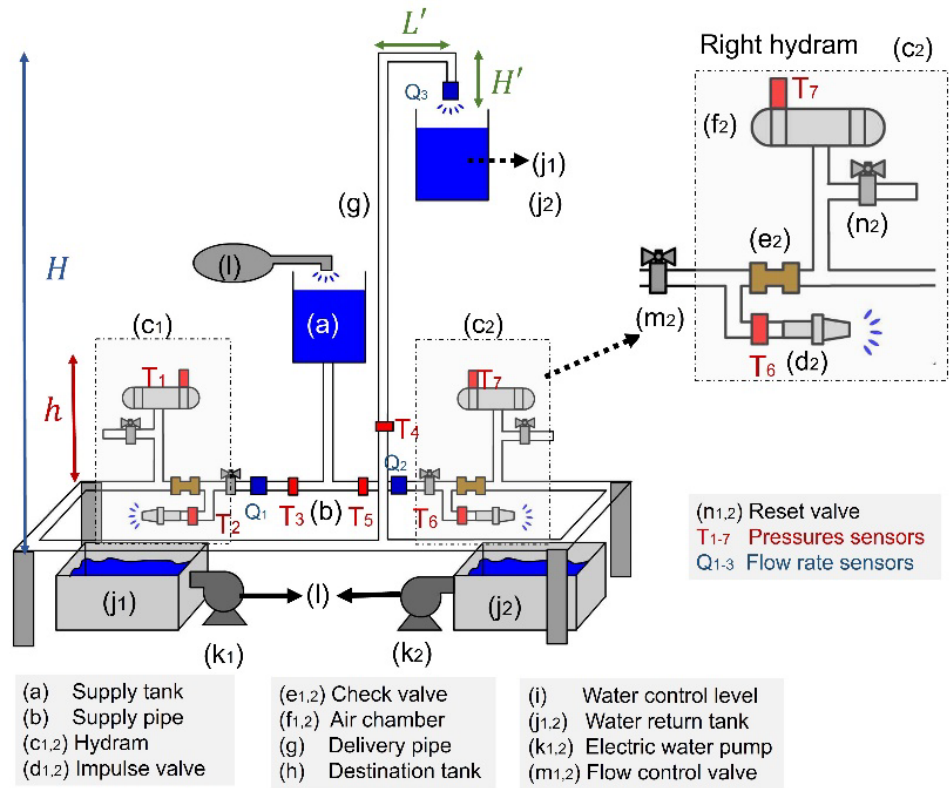
1. Supply, starts in the supply tank (a) as a vertical pipeline with diameter of 0.0508 m and a height of 1.3 m, and is divided into two pipes with diameters of 0.0258 m and a length of 1 m through a T joint that supplies the flow for the two rams (d_1 , d_2).

2. Elevation, reuses the water from the discharge tanks (j_1 , j_2) to the supply tank (a) by means of two radial pumps (k_1 , k_2).

3. Delivery, starts as two horizontal pipes with a diameter of 0.0254 m and a length of 0.30 m which are attached to the output of the air chambers (f_1 , f_2), and have perpendicular trajectories that change the flow direction a length of 1 m in the horizontal plane, and finally they are coupled to a T-joint with the same diameter. A vertical pipeline with a length of 6 m is coupled to the outlet of the T-joint. At the highest level of the vertical pipeline and additional pipe (L') of 0.20 m length and 0.0254 m in diameter is coupled with two perpendicular joints (at each side). At the end of this, a downward-vertical pipeline is coupled. Thus, the delivery pipe has a U-shape that returns the flow in a downward direction. This downward pipe is what we have called the return-pipe. To guarantee the speed of the supplied flow rate, two flow control valves (m_1 , m_2) were used.



(a)



(b)

Figure 4. Experimental setup: (a) photo, and (b) schematic with their respective measurement systems and locations.

Instrumentation and measurement

The supplied flow rates were measured using two Doppler effect flowmeters (Greyline Instruments Inc, DFM 5.0, Birmingham, UK), located in their respective supply pipes. The pumped flow rates were measured with a turbine flowmeter (EDM, Kobold, Perú) located at the end of the of the vertical delivery pipeline.

The pressure was measured using seven transducers (Danfoss, MBS1900, Nordborg, Denmark), that were located at the points of interest in the hydraulic circuit, namely, in the impulse valves (2 sensors), the horizontal supply pipes (2 sensors), the air chambers (2 sensors), and in the delivery pipe (1 sensor). The pressure transducers are piezoresistive devices that operate with an input voltage between 9 and 28 V and provide output signals between 4-20 mA. The pressure range is between 0 and 25 bars (0-2500 kPa). Transducers are labeled from T1 to T7, as shown in Figure 3.

The pressure sensors were attached to pipes by means of a plastic collar with a hole concentric to holes in the pipeline. Holes in the pipelines were carefully machined to avoid imperfections that may convert velocity energy into pressure energy (Figure 5).



Figure 5. Flexible coupling to attach pressure transducers to hydraulic pipes.

The pressure sensors were calibrated using a manometer (Omega, DPG4000, Omega Engineering Inc., USA), as shown in Figure 6. During the calibration, the sensor holder tube was supplied with pressurized air and the pressure was sensed by the transducers and measured with the reference manometer.

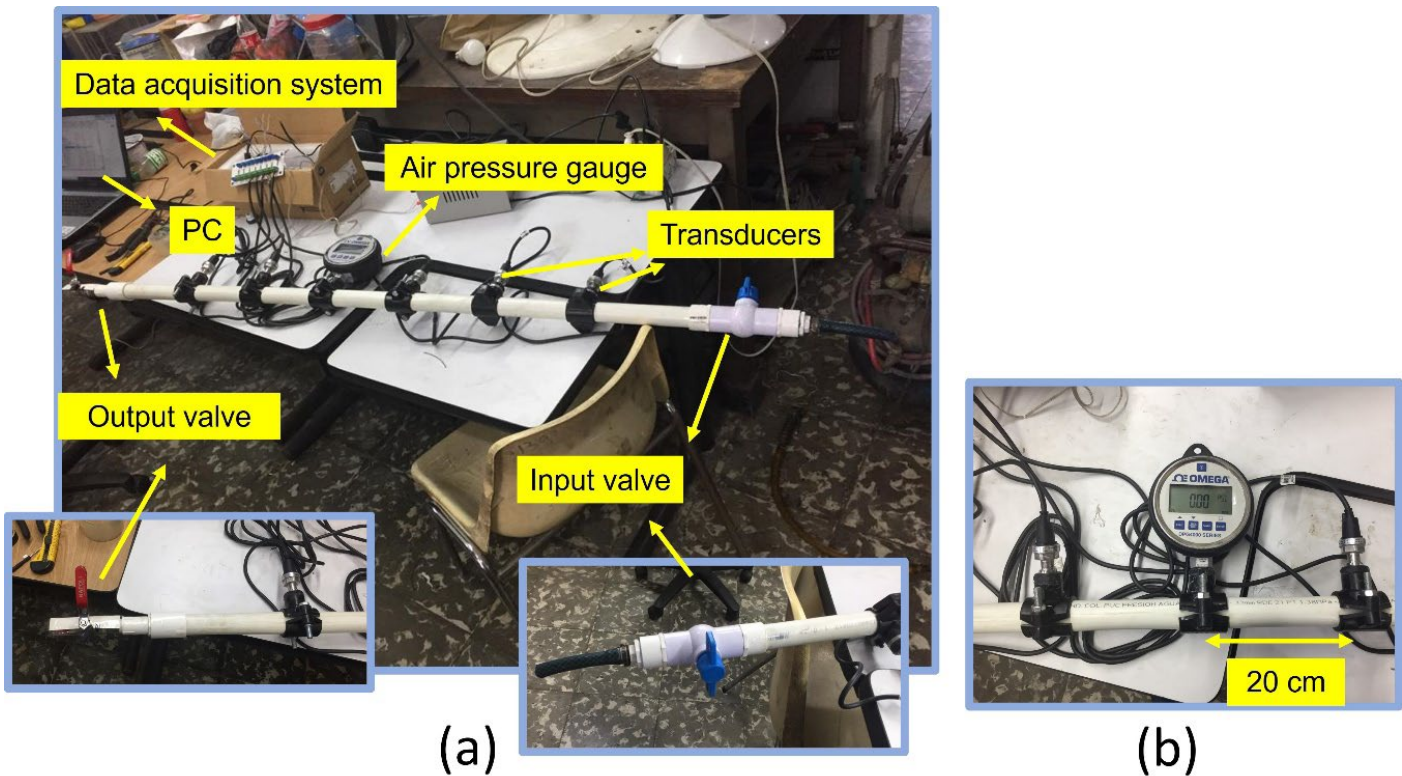


Figure 6. (a) Calibration system composed of a pipe with attached transducers and, (b) air pressure gauge.

Signals measured were processed to obtain the calibration curve of the pressure transducers, as well as the error in the pressure measurement, as presented in Figure 7.

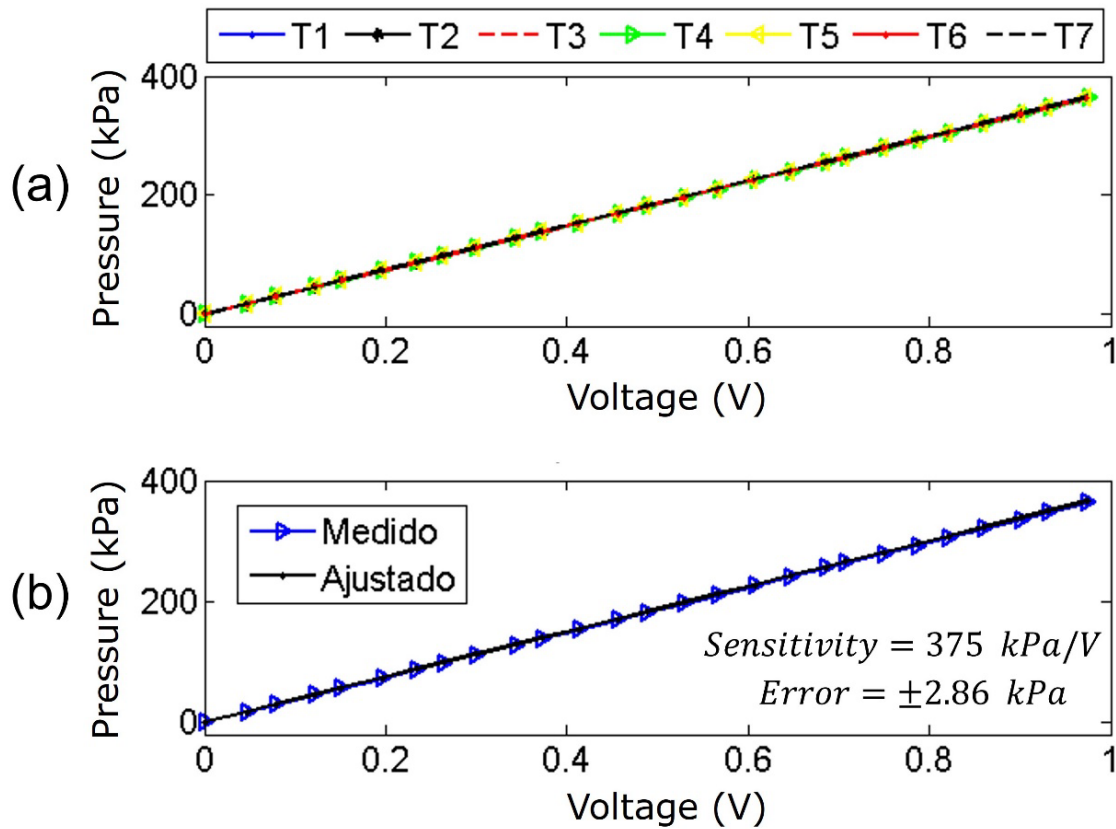


Figure 7. (a) Curves of Voltage vs. pressure for the seven pressure transducers used, and (b) sensitivity curves of pressure transducers.

Figure 8 depicts a block diagram that synthesizes the experimental procedure for data acquisition.

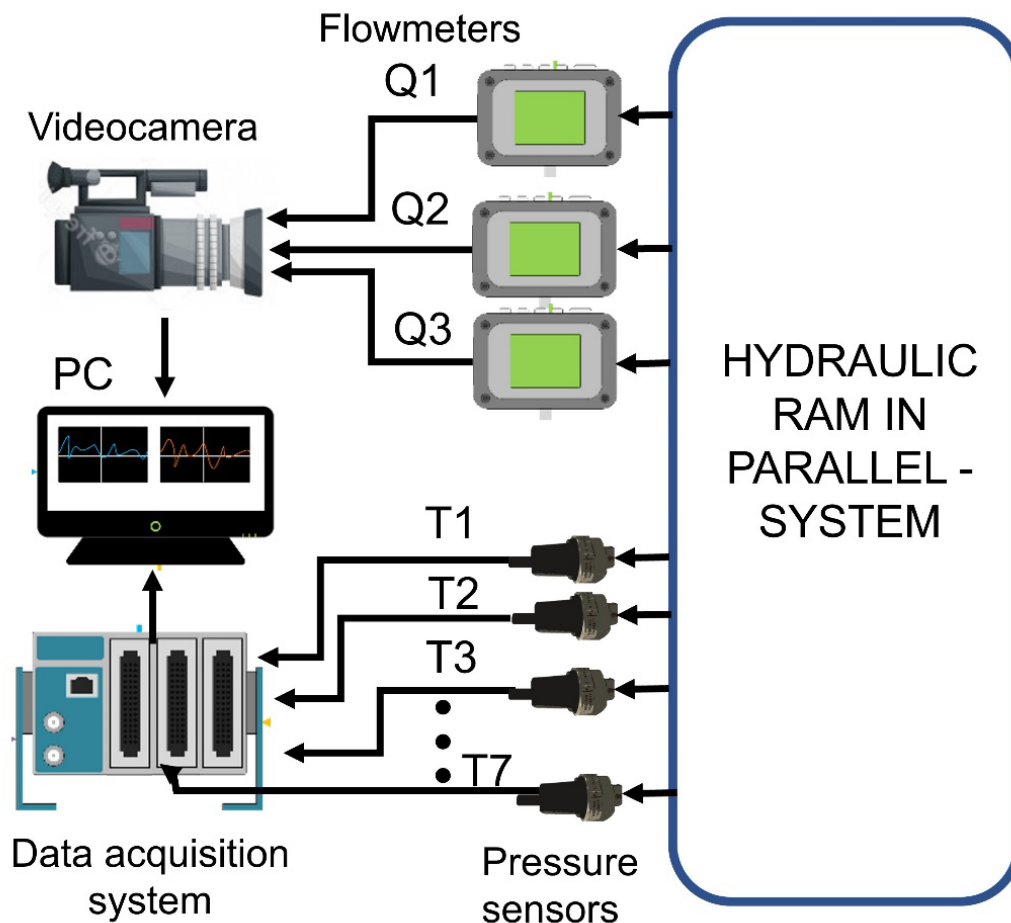


Figure 8. Schematic of the implemented acquisition system to measure flow rates and pressure.

For the analysis, a linear fitting under the following parameters was considered: SSE: 0.02423, R-square: 1, RMSE: 0.03113. The maximum calibration error obtained was ± 7.6353 mV, equivalent to 0.4118 psi (2.83 kPa), and the sensitivity of the transducers is $p(\text{kPa}) = 375 \text{ kPa/V}$.

The pressure measured were captured by means of a data acquisition chassis (Model CDAQ 9178, National Instruments, USA), and

two modules (Model 9215, National Instruments, USA) with 4 analog inputs each. The data processing consists of implementing the short-time fast Fourier transform to obtain the frequency components of the water hammer.

The flow rates were provided by the flowmeters were recorded by a videocamera at a rate of 60 fps. For each experiment, the video was processed to obtain the lectures of the flowmeters with a duration of four minutes (240 s). The software used was MatLab.

Methodology

A verification of the proper operation of impulse valves was performed and the length of the compressed spring at which each hydraulic ram delivers the highest pumped flow rate was determined (Figure 9). This includes the condition where each impulse valve automatically starts. Under this condition, the closing speed (controlled by the flow control valves) without varying the opening of the control valve was calculated. All tests were performed using the control valve totally opened since this is the condition where the maximum pumped flow rate is achieved.

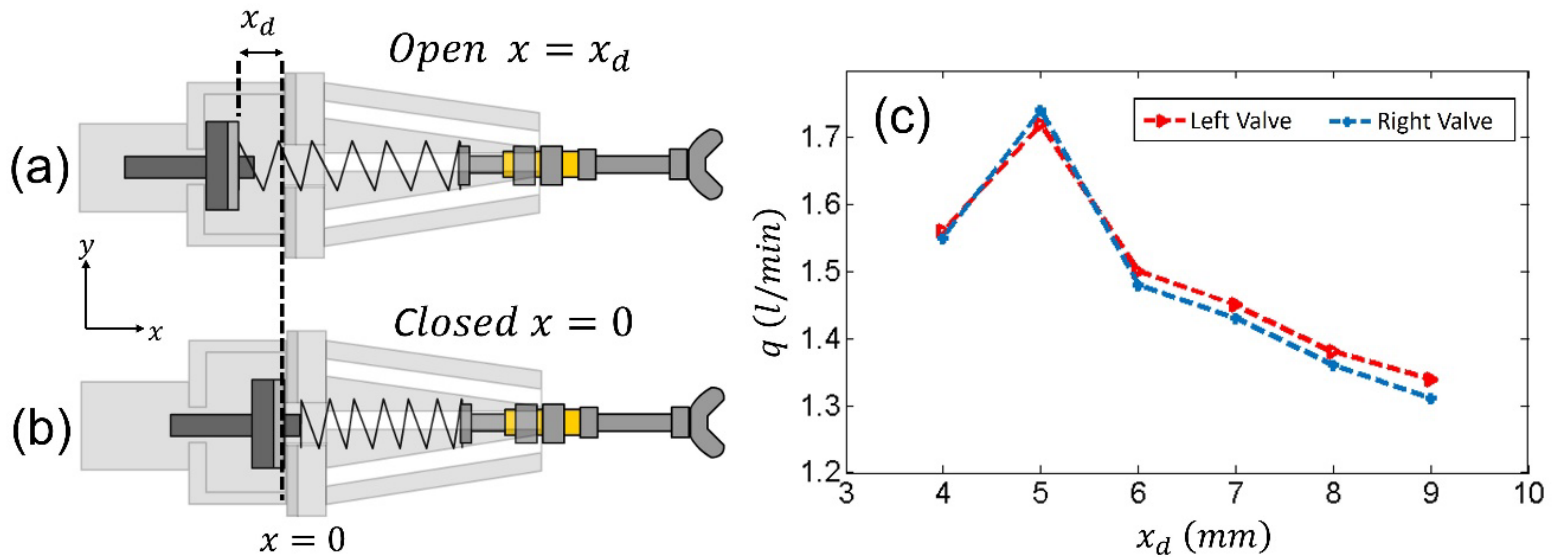


Figure 9. Schematic of the impulse valve (a) open and (b) closed. (c) Delivered or pumped flow rate (q) vs spring compression distance (x_d).

Tests were carried out with three supply heights (h) of 1.5, 1.7, and 1.9 m. The latter is the maximum water level of the supply tank. The depth of the supply tank is 1 m and it is at a height of 1.3 m from the level of the rams. The maximum flow experimentally obtained is delivered when the springs of the rams are compressed 0.0875 m. For each test, the initial volume of the supply tank was firstly set up. To guarantee a constant volume of the supply tank, five lateral valves attached to the supply tank at different heights controlled the flow rate. The height between these vertical valves is 0.1 m and the lowest valve was located at 1.5 m measured from the rams' locations. Once the supply height is set up, the flow rates were measured for 240 s (4 minutes) without (at a delivery height of 6 m) and with the return-pipe. Under these two configurations, the delivered flow rate was addressed to the supply tank

in order to reuse this water. Next, the pressure signals in the delivery pipe, near each hydraulic ram, in the air chambers, and at the beginning of the vertical supply pipe were recorded. Figure 10a shows the characteristic pressure signals provided by sensors T2 and T3. Figure 10b shows the influence of the opening angle of the flow control valve on the delivery flow rate. Also, the time of flight of the pressure wave can be calculated using the time that takes the wave to go from sensor T2 to T3, as illustrated in Figure 10c. Finally, the characteristic curves in the air chamber for three different tests at different supply heights $h = 1.5, 1.7$, and 1.9 m, as presented in Figure 10d).

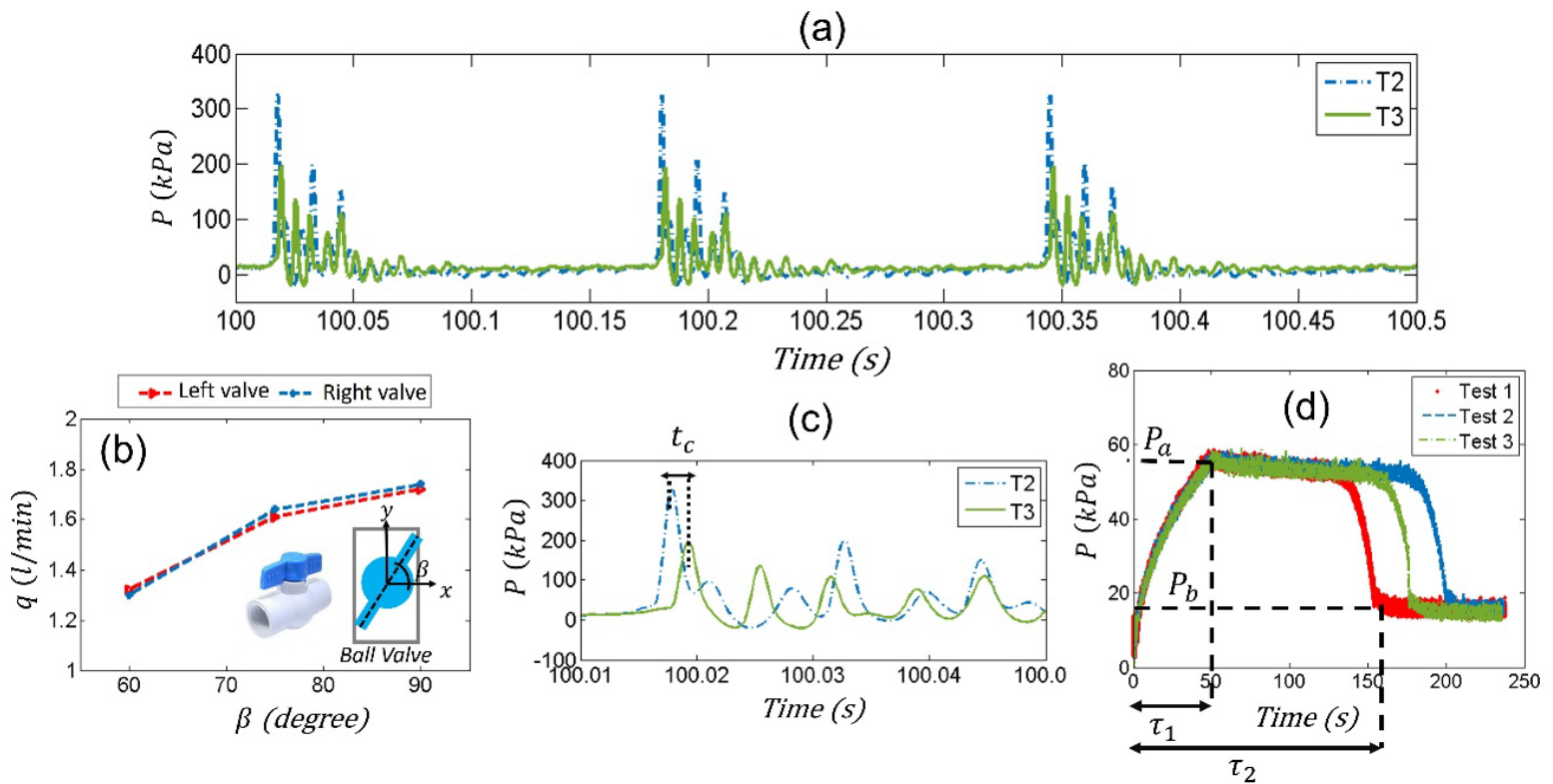


Figure 10. (a) Measured pressure signals near the left hydram arm (T2) and at its respective supply pipe (T3); (b) open angle (β) of the ball valve; (c) time of flight of the pressure wave measured between T2 and T3, and (d) pressure signals at the left air chamber for three different tests.

The operation of the hydraulic circuit with a single ram involved completely the opening of the flow control valve on one arm of the circuit and the total closing of the flow control valve on the other arm. For the operation of the hydraulic rams in parallel, both flow control valves were fully opened. Once the initial conditions were set up, the pressure and the flow rates were recorded.

Results

The performance of the proposed configurable hydraulic system was evaluated by measuring the flow rates and the pressure at different locations, under different supply heights (h) and only one delivery height (H). These variables were recorded for both configurations: when the circuit is operated with 1) a single ram, and 2) two rams operating simultaneously.

Single hydraulic ram operating with vertical-horizontal downward supply pipe, with and without return pipe

The fourth and fifth column in Table 1 presents the pressure (F_p) at the air chamber, the water hammer frequency (F_p), and the pumped flow rate (q) when a single ram is operating during 240 s.

Table 1. Pressure in the air chamber P , water hammer frequency F_p , and pumped flow rated q using a single hydraulic ram for supply heights h of 1.5, 1.7 y 1.9 m.

			With return-pipe	Without return-pipe
		$t < \tau_1$	$\tau_1 \leq t < \tau_2$	$t > \tau_2$
$h = 1.50 \text{ m}$ $\tau_1 = 113.80 \text{ S}$ $\tau_2 = \infty \text{ S}$	$P(\text{kPa})$	---	55.03	55.03
	$F_p \text{ (Hz)}$	---	5.53	5.53
	$q \text{ (l/min)}$	0.00	1.10	1.10
	$\Delta P = P_{T2} - P_{T1} \text{ (kPa)}$	---	268.97	268.97
$h = 1.70 \text{ m}$ $\tau_1 = 82.55 \text{ S}$ $\tau_2 = \infty \text{ S}$	$P(\text{kPa})$	---	55.03	55.03
	$F_p \text{ (Hz)}$	---	6.03	6.03
	$q \text{ (l/min)}$	0.00	1.30	1.30
	$\Delta P = P_{T2} - P_{T1} \text{ (kPa)}$	----	261.57	261.57
$h = 1.90 \text{ m}$ $\tau_1 = 67.92 \text{ S}$ $\tau_2 = \infty \text{ S}$	$P(\text{kPa})$	---	55.03	55.03
	$F_p \text{ (Hz)}$	---	6.75	6.75
	$q \text{ (l/min)}$	0.00	1.73	1.73
	$\Delta P = P_{T2} - P_{T1} \text{ (kPa)}$	-----	224.97	224.97

Figure 11 present the delivered or pumped (q), supplied (Q_t) and wasted (Q) flow rates for supply heights $h = 1.5, 1.7$ y 1.9 m .

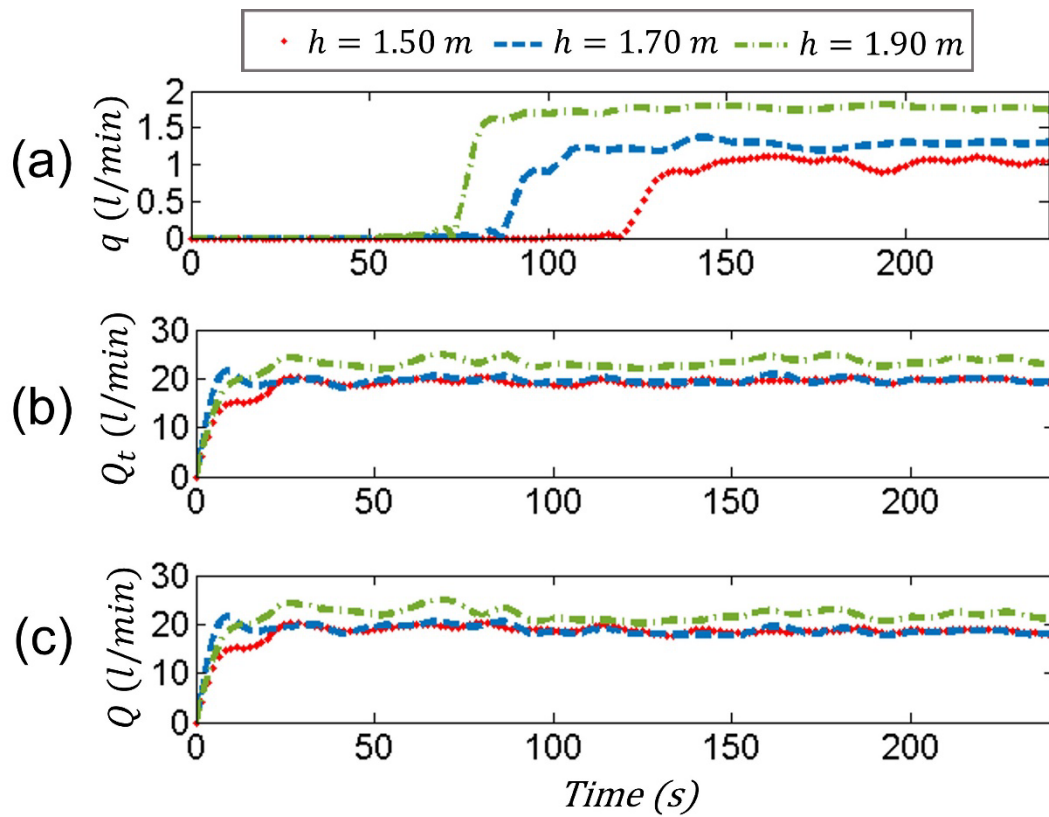


Figure 11. (a) Delivered (q), (b) total (Q_t), and (c) wasted (Q) flow rates for a single hydram with a single-vertical supply pipe.

Figure 12 shows the pressure signals in the impulse pipe (T3) and near the left hydram arm (T2) for supply heights $h = 1.5$, 1.7 y 1.9 m .

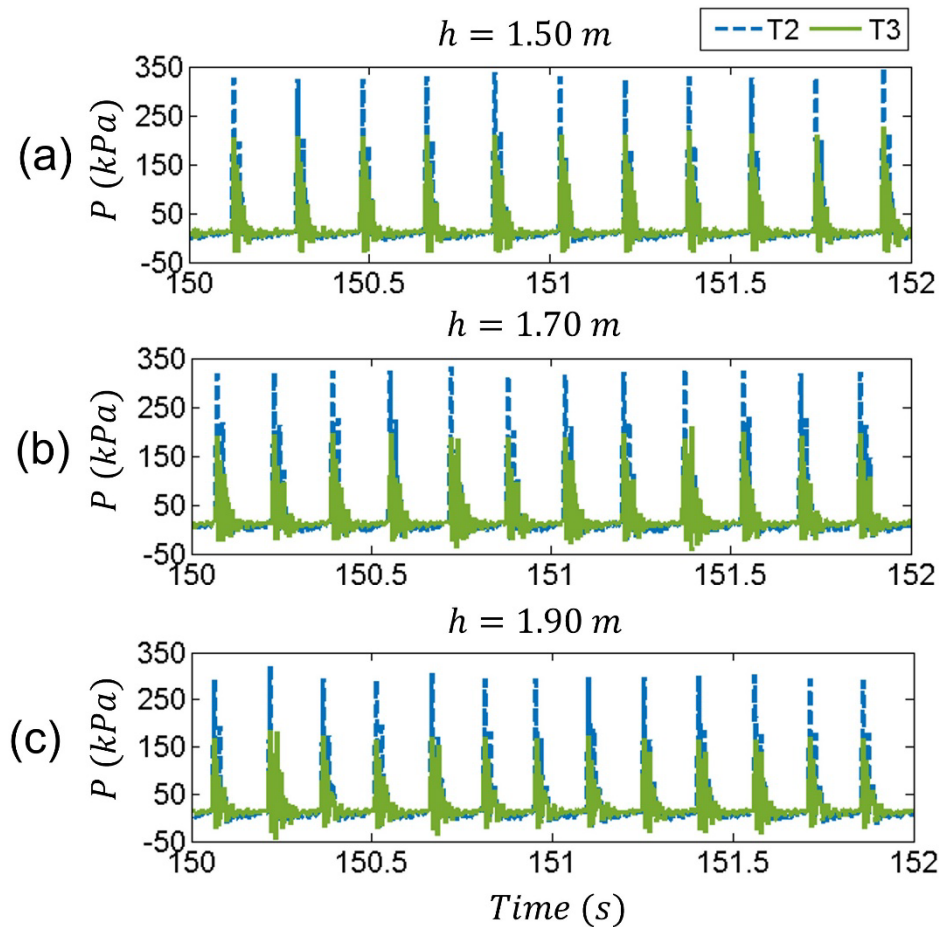


Figure 12. Pressure signals at supply pipe (T3) and near the left hydram arm (T2) for three different supply heights $h = 1.50, 1.70$ y 1.90 m with vertical return-pipe.

Figure 13a describes the pressure in the air chamber of the studied ram during 240 s captured by the sensor (T1) and at the beginning of the delivery pipe obtained by sensor (T4). It is observed that while the pressure in T4 presents considerable oscillations due to the water hammer, in the air chamber (T1) the pressure is damped and is equal to the static pressure associated with the delivery height. Figure 13b-d describe the

pressure signal at the beginning of the delivery line (T4) for 2 seconds in the steady state for the three supply heights tested. The pressure difference $\Delta P = P_{T2} - P_{T1}$ between the left ram (T2) and its air chamber (T1), respectively, is shown in Table 1.

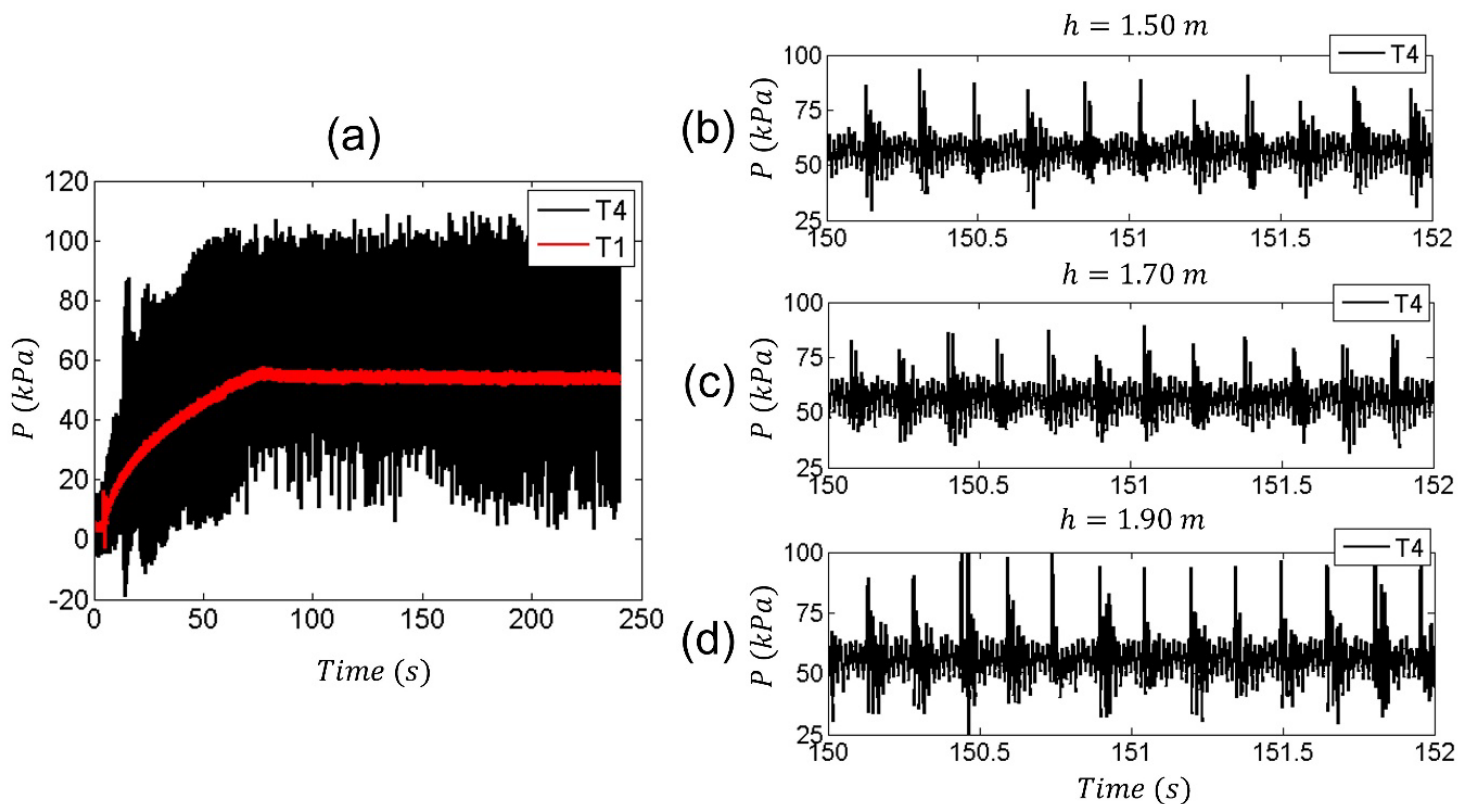


Figure 13. (a) Pressure signals at air chamber (T1) and supply pipe (T4) for (b) $h = 1.5$ m, (c) $h = 1.7$ m, and (d) $h = 1.9$ m.

Figure 14 describes the behavior over time of: a) pressure (P) in the air chamber, b) water hammer frequency (F_p), c) delivered flow rate (q), and d) the efficiency (η) of the hydram.

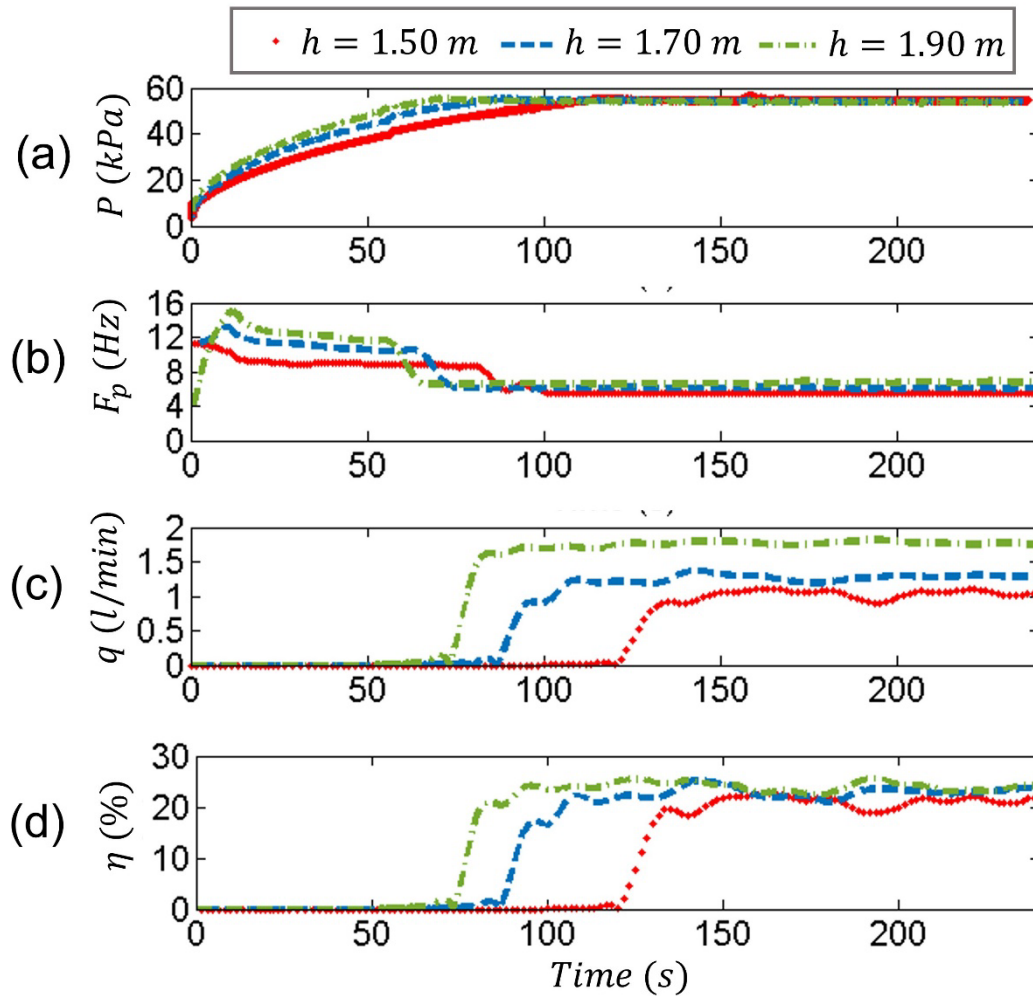


Figure 14. (a) Pressure and (b) frequency of the water hammer measured at the left hydram arm; (c) delivered flow rate, and (d) efficiency of the single ram.

Two-armed hydraulic ram operating in parallel with vertical-horizontal downward supply pipe, with and without return pipe

The operation to the rams in parallel with vertical-radial supply was set up by opening fully both control valves. With this configuration, the same variables of interest were measured. Results are presented in Table 2.

Table 2. Pressure in the air chamber P , water hammer frequency F_p , and pumped flow rated q using two-armed hydraulic ram in parallel for supply heights h of 1.5, 1.7 y 1.9 m.

			With return- pipe	Without return-pipe
		$t < \tau_1$	$\tau_1 \leq t < \tau_2$	$t > \tau_2$
$h = 1.5 \text{ m}$ $\tau_1 = 57.69 \text{ s}$ $\tau_2 = \infty \text{ s}$	$P(\text{kPa})$	53.48	55.03	55.03
	$F_p \text{ (Hz)}$	---	4.90	4.90
	$q \text{ (l/min)}$	0.00	2.26	2.26
	$\Delta P = P_{T2} - P_{T1} \text{ (kPa)}$	---	266.32	266.32
$h = 1.7 \text{ m}$ $\tau_1 = 49.39 \text{ s}$ $\tau_2 = 199.4 \text{ s}$	$P(\text{kPa})$	----	55.03	15.50
	$F_p \text{ (Hz)}$	----	5.8	12.40
	$q \text{ (l/min)}$	0.00	2.60	11.70
	$\Delta P = P_{T2} - P_{T1} \text{ (kPa)}$	----	274.97	314.5.12
$h = 1.9 \text{ m}$ $\tau_1 = 41.17 \text{ s}$ $\tau_2 = 62.99 \text{ s}$	$P(\text{kPa})$	----	53.48	17.55
	$F_p \text{ (Hz)}$	-----	6.75	14.65
	$q \text{ (l/min)}$	0.00	3.40	13.20
	$\Delta P = P_{T2} - P_{T1} \text{ (kPa)}$	-----	226.52	262.45

Figure 15 describes the pressure before and near the rams, captured by the pressure sensors (T3) and (T2), respectively. Under these conditions it was observed that the frequency of the water hammer in the delivery valve increases as the supply height increases. Also, the magnitude of the pressure in the impulse pipe slightly decreases as the supply height increases. However, the pressure in the delivery pipe is greater than when a single ram operates. It is worth mentioning the automatic operation of the impulse valve that does not require an initial impulse to start its operation.

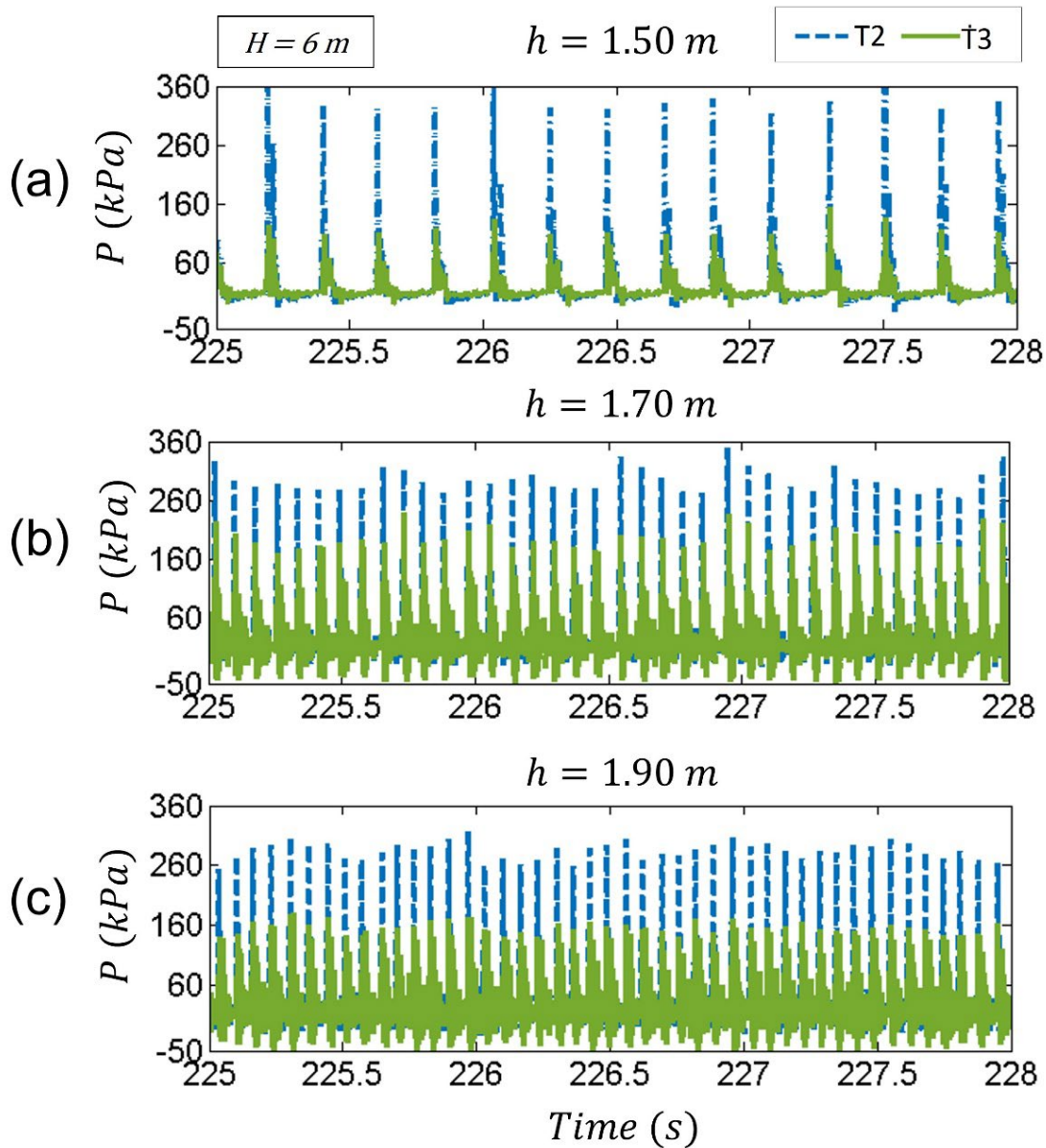


Figure 15. Pressure signals at supply pipe (T3) and near the left hydram arm (T2), of a two-armed ram in parallel with vertical return-pipe for three different supply heights (a) $h = 1.50$ m, (b) $h = 1.70$ m, and (c) $h = 1.90$ m.

The evolution of the delivered (q), wasted (Q), and total (Q_t) flow rates for the three supplied heights (h) evaluated during 240 s is presented in Figure 16. For $h = 1.7$ m is notorious the effect of the return-pipe in the delivered flow. Also, it can be observed that the wasted and total flow rates present a similar behavior.

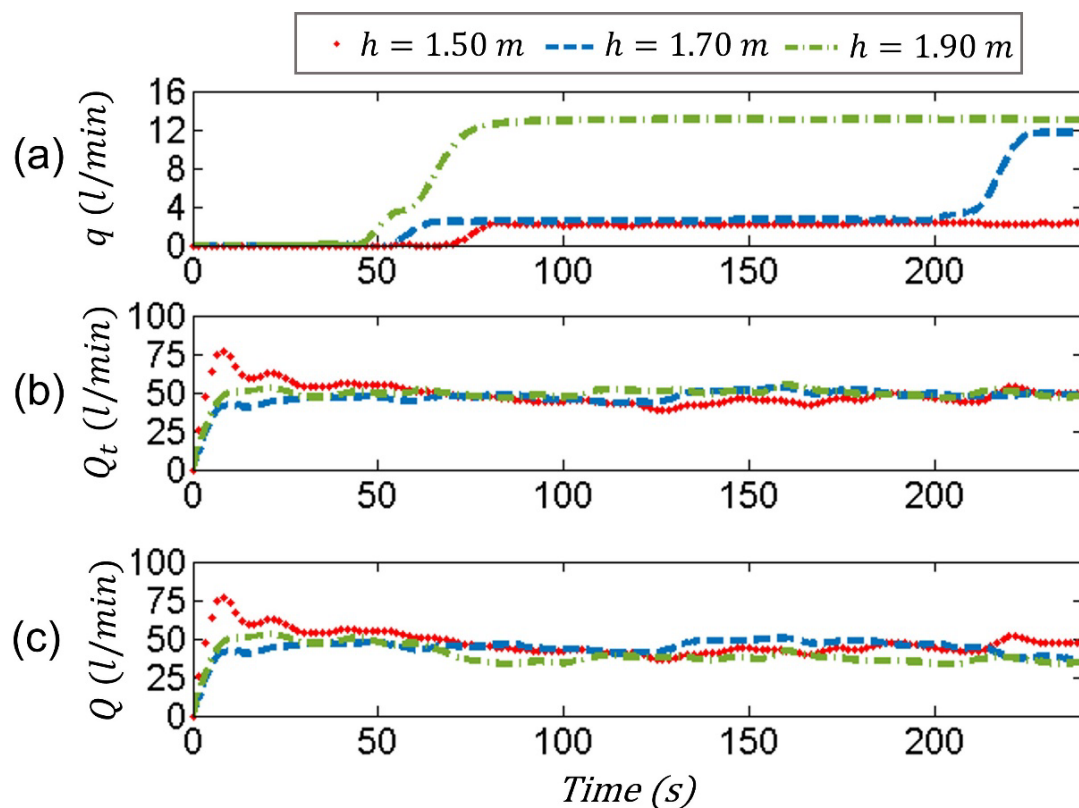


Figure 16. (a) Delivered (q); (b) total (Q_t), and (c) wasted (Q) flow rates for a two-armed hydram with return pipe at three different height $h = 1.5$, 1.7 , and 1.9 m.

The behavior of the pressure in the air chamber, the frequency of the water hammer, the pumped flow rates, and the efficiency of two armed-hydraulic rams operating in parallel are illustrated in Figure 17. It is observed that the return pipe does not affect the pressure in the air chamber when the supply height is 1.5 m. The effect is evident with the supply height of 1.7 m where the pressure in the air chamber decreases approximately 150 s later in comparison with the behavior when the supply height is 1.9 m. Evidently, the pressure drop in the air chamber appears when the water reaches a height of 6 m in the delivery pipe and causes the water hammer frequency to increase from 4 Hz to 15 Hz. Figure 18d shows the efficiency of the hydram, where the increase in the flow rate is observed due to the effect of the return pipe that occurs for supply height $h = 1.70$ and 1.90 m.

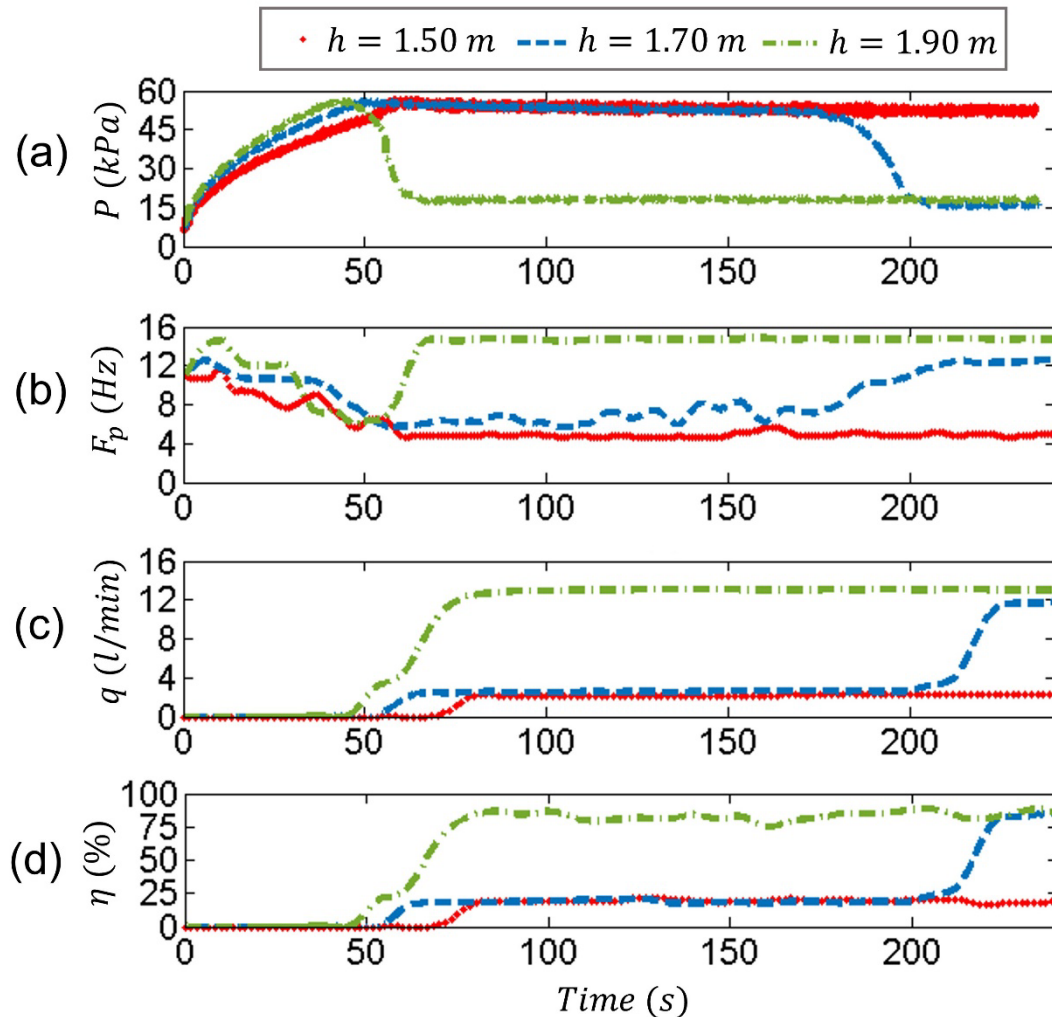
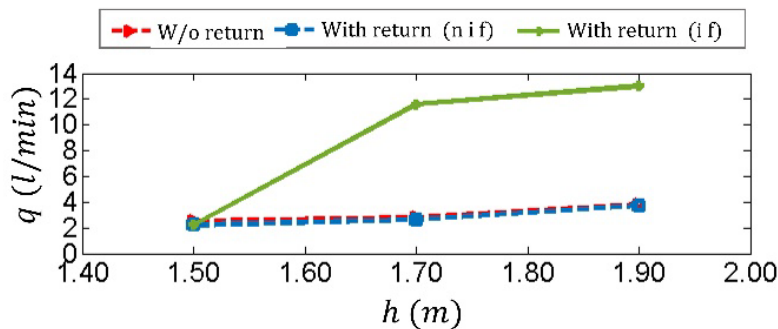


Figure 17. (a) Pressure and (b) frequency of the water hammer measured at the left hydram arm; (c) delivered flow rate, and (d) efficiency of two-armed hydram operating in parallel configuration.

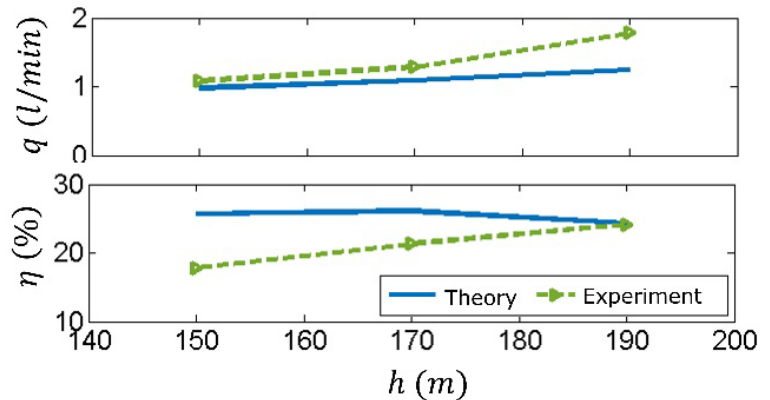
Figure 18a compares the pumped flow rate for three different cases, namely: 1) without return pipe where it was observed that the flow did not increase (w/o return), 2) with return pipe and with flow that does not increase (w return and no increased flow), and 3) with return pipe and

the flow increases (with return and increased flow). Figure 18b shows the efficiency of the pumping system. For heights $h = 1.70$ and 1.90 m the delivered flow increases because of the return-pipe.

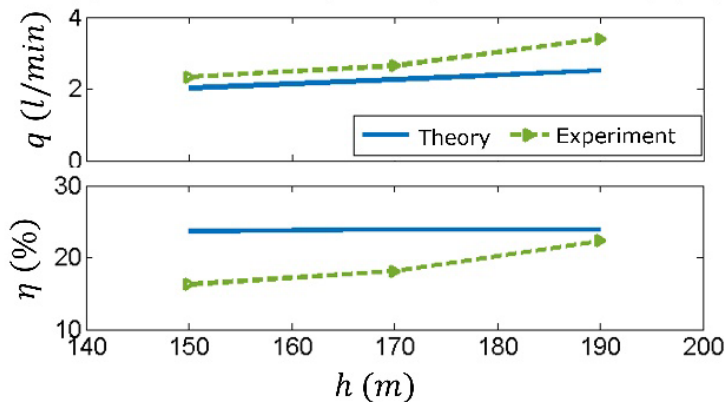
(a)



(b) Single hydram (with return pipe)



(c) Two-armed hydram (without return pipe)



(d) Two-armed hydram (with return pipe)

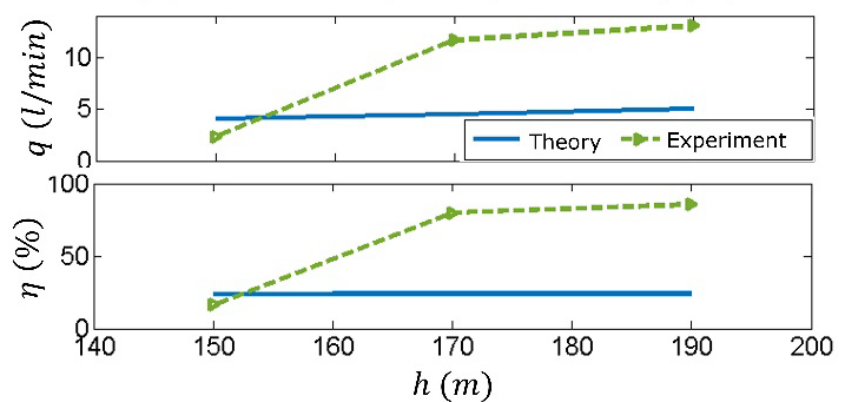


Figure 18. Effect of the return pipe on the flow rate behavior for two-armed hydram connected in parallel. Flow rate and efficiency of the configuration (b) single hydram with return pipe, and two-armed hydram in parallel (c) without return pipe and (d) with return pipe.

Finally, results from theory and experiments are compared for a single ram with return-pipe (Figure 18b), with two-armed hydram operating in parallel without the return-pipe (Figure 18d), and with return-pipe (Figure 18e).

Discussion

Similar to radial pumps connected in parallel, Table 1 and Table 2 indicate that two hydraulic rams with vertical-radial supply and delivery pipelines in parallel provides more water than a single ram, but less than the sum of the flow rate that they provide with independent delivery pipes. In addition, the pressures in the delivery pipeline and near each hydraulic ram show that the frequency of the water hammer for a single ram is lower than that for two rams in parallel. This behavior is preserved for different delivery heights (h) evaluated.

Also, by increasing the supply height, the pumped flow rates increase. However, for a two-armed hydraulic ram, this effect occurs with different start times (Figure 11 and Figure 16). Furthermore, at least with $h = 1.7$ m and $h = 1.9$ m, the return-pipe affects the pressure difference between the hydraulic rams in parallel and their air chambers, as observed in Tables 1 and 2. This result was validated by the behavior of the pressure in the air chamber for different delivery heights, as presented in Figure 14a and Figure 17a. Similarly, with the aim to evaluate the Tacke (1988) model to predict the delivered flow rate by a single hydraulic ram, this variable was estimated and compared with those measured in the laboratory with the two circuit configurations.

Therefore, by adding the return-pipe the divergence is significant, as shown in Figure 18e. Also, a system with two hydraulic rams in parallel has a higher efficiency (Figures 18 b and d).

Finally, Table 3 provides the delivered flows reported by several authors using different rams and presents a comparison between the order of magnitude obtained by them and in this work. In addition, is important to mention that the increase of the flow rate is significant when the return-pipe is considered.

Table 3. Delivered flow rates reported for different hydraulic rams.

Reference	h (m)	H (m)	D (m)	D (m)	$L_I(m)$	$L_E(m)$	F (Hz)	Q_s (l/)	Q_E (l/s)
Suarda <i>et al.</i> (2020)	1.8	2.020	0.0320	0.0120	12.2	1.36		0.280	0.0120
Girish, Naik, Prakash and Kumar (2016)	1.0	1.475	0.0254	0.0254	5.0			0.2330	0.0540
Arangurí-Cayetano (2018)	1.75	5.0	0.0508	0.0254			2.1	1.175	0.0742
This research*	1.9	6.0	0.0254	0.0254	1.5	6.0	8.89	0.42	0.0283

*Delivered flow rate with return pipe 0.1482 l/s (Table 1).

Conclusions

This work presents the design and fabrication of a hydraulic circuit with the capacity to be operated in both configurations: with 1) single, and 2) two armed-hydraulic rams with vertical-radial supply and independent parallel discharge. In both cases, an additional return-pipe (downpipe) was attached just at the highest delivery height to return the flow a desired distance. The aim of this study was to investigate the performance of the hydraulic circuit to evaluate the feasibility of a system of multiple hydraulic with an alternative configuration composed of a vertical-radial supply pipe and parallel discharge. Flow rates, as well as pressures at different points of the circuit were measured. Thus, a comparison between both configurations determined the best operating condition. Additionally, the following experimental results were obtained:

1. The proper operation of a single and two-armed rams with and without a return-pipe (downpipe) when the supply pipe has a vertical-radial configuration.
2. The experimental information compares the performance of a single and two-armed hydraulic rams operating in parallel under the same supply heights.
3. Equivalently to radial pump devices, the flow pumped by two rams in parallel is higher than that of a single ram, but less than the sum of the flow rates delivered by each of them.
4. The reduction of a vertical descending section attached to the delivery pipe significantly increases the pumped flow if the delivery pipe has a return at a height greater than the level of the supply tank.

5. The effect of the return-pipe may be associated to the acceleration of the flow in the descending section, which directly depends on the height of the return-pipe.
6. An alternative configuration pumping system was presented with a high potential to delivery water to communities located in places with devious and abrupt topography.
7. This study paves the way to the development of alternative and green technologies based on multiple hydraulic rams.

Acknowledgement

E.R.M. acknowledges support from Universidad del Valle research project CI 21080. In honor of the memory to E.R.M. wife.

References

- Alrikabi, N. Kh. M. A. (2014). Renewable energy types. *Journal of Clean Energy Technologies*, 2(1), 61-64.
- Arangurí-Cayetano, D. J. (2018). *Efectividad del sistema de bombeo con ariete hidráulico en la zona rural de la provincia de San Pablo-Cajamarca* (tesis de doctorado no publicada). Universidad Nacional de Cajamarca. Recovered from <https://repositorio.unc.edu.pe/bitstream/handle/20.500.14074/2138/Efectividad%20del%20Sistema%20de%20Bombeo%20con%20Ariete%20Hidr%C3%A1ulico%20en%20la%20Zona%20Rural%20de%20La%20Provincia%20de%20San%20P.pdf?sequence=1&isAllowed=y>

- Arapa-Quispe, J. B. (2016). Evaluación del rendimiento del ariete hidráulico Bah-1.1/2 variando la longitud de la tubería de alimentación y condiciones de operación de la válvula de impulso. *Anales Científicos*, 77(2), 155. DOI: <https://doi.org/10.21704/ac.v77i2.485>
- Cahill, A. E., Aiello-Lammens, M. E., Caitlin-Fisher-Reid, M., Hua, X., Karanewsky, C. J., Ryu, H. Y., Sbeglia, G. C., Spagnolo, F., Waldron, J. B., Warsi, O., & Wiens, J. J. (2013). How does climate change cause extinction? *Proceedings of the Royal Society B: Biological Sciences*, 280(1750). DOI: <https://doi.org/10.1098/rspb.2012.1890>
- Credo, M. C., & Metra, D. P. (2020). Design analysis, installation and performance evaluation of a hydraulic ram pump system with a modified waste valve. *Vietnam Journal of Science and Technology*, 58(1), 107.
- De-Carvalho, M. O. M., Diniz, A. C. G. C., & Neves, F. J. R. (2011). Numerical model for a hydraulic ram pump. *International Review of Mechanical Engineering*, 5(4), 733-746.
- DTU. (1996). *New developments in hydraulic ram pumping*. Recovered from <https://warwick.ac.uk/fac/sci/eng/research/grouplist/structural/dtu/pubs/tr/lift/rptr13/>
- El Zein, A. L., & Chehayeb, N. A. (2015). The effect of greenhouse gases on Earth's temperature. *International Journal of Environmental Monitoring and Analysis*, 3(2), 74. DOI: <https://doi.org/10.11648/j.ijema.20150302.16>

- Filipan, V., Virag, Z., & Bergant, A. (2003). Mathematical modelling of a hydraulic ram pump system. *Strojniski Vestnik/Journal of Mechanical Engineering*, 49(3), 137-149.
- Ghidaoui, M. S., Zhao, M., McInnis, D. A., & Axworthy, D. H. (2005). A review of water hammer theory and practice. *Applied Mechanics Review*, 58(1), 49-76. DOI: <https://doi.org/10.1115/1.1828050>
- Girish, L. V., Naik, P., Prakash, H. S. B., & Kumar, M. R. S. (2016). Design and fabrication of a water lifting device without electricity and fuel. *International Journal on Emerging Technologies*, 7(2), 112-116.
- Glover, P. B. M. (1994). *Computer simulation and analysis methods in the development of the hydraulic ram pump*. Coventry, UK: University of Warwick.
- IDRC-MR102eR. (1986). *Proceedings of a Workshop on Hydraulic Ram Pump (Hydrum) Technology*. Ottawa, Canadá: Centro Internacional de Investigaciones para el Desarrollo.
- Iversen, H. W. (1975). An analysis of the hydraulic ram. *Journal of Fluids Engineering, Transactions of the ASME*, 97(2), 191-196. DOI: <https://doi.org/10.1115/1.3447251>
- Jafri, M., & Sanusi, A. (2019). Analysis effect of supply head and delivery pipe length toward the efficiency hydraulic ram 3 inches. *International Research Journal of Advanced Engineering and Science*, 4(2), 263-266.

- Januddi, F. S., Huzni, M. M., Effendy, M. S., Bakri, A., Mohammad, Z., & Ismail, Z. (2018). Development and testing of hydraulic ram pump (hydram): Experiments and simulations. *IOP Conference Series: Materials Science and Engineering*, 440(1). DOI: <https://doi.org/10.1088/1757-899X/440/1/012032>
- Krol, J. (1947). *A critical survey of the existing information relating to the automatic hydraulic ram pump (London University)*. Recovered from <https://openresearch.surrey.ac.uk/esploro/outputs/doctoral/A-critical-survey-of-the-existing/99514364202346#file-0>
- Kimaro, S. J., & Salaam, D. (2018). The influence of air vessel volume on the delivery flow rate and efficiency of a hydram water pumping system. *International Research Journal of Engineering and Technology*, 5, 1312-1320.
- Kweku, D., Bismark, O., Maxwell, A., Desmond, K., Danso, K., Oti-Mensah, E., Quachie, A., & Adormaa, B. (2018). Greenhouse effect: Greenhouse gases and their impact on global warming. *Journal of Scientific Research and Reports*, 17(6), 1-9. DOI: <https://doi.org/10.9734/jsrr/2017/39630>
- Lansford, W. M., & Dugan, W. G. (1941). *An analytical and experimental study of the hydraulic ram*. Champaign, USA: University of Illinois at Urbana Champaign, College of Engineering.
- Manzini, F., Islas, J., & Martínez, M. (2001). Reduction of greenhouse gases using renewable energies in Mexico 2025. *International Journal of Hydrogen Energy*, 26(2), 145-149. DOI: [https://doi.org/10.1016/S0360-3199\(00\)00042-2](https://doi.org/10.1016/S0360-3199(00)00042-2)

- Najm, H. N., & Azoury, M. P. (1999). Numerical simulation of the hydraulic ram: A new look at an old device. A01198 © IMechE 1999. *Proceedings of the Institution of Mechanical Engineers*, 213(Part A, 213), 127-141.
- Ngolle, E. E. G., & Hong, S. G. (2019). Experimental study on the effect of air chamber size and operation parameters on the performance of a hydraulic ram pump. *Journal of the Korean Society of Agricultural Engineers*, 61(4), 55-61. DOI: <https://doi.org/10.5389/KSAE.2019.61.4.055>
- Pramono, B. A., Suharno, K., & Widodo, S. (2018). Analisis efisiensi pompa hidram paralel empat dengan diameter katup buang 1 inchi dan 1 1 / 4 inchi berdasarkan variasi pipa inlet. *Jurnal Teknik Mesin MERC (Mechanical Engineering Research Collection)*, 1(2). Recovered from https://www.semanticscholar.org/paper/ANALISIS-EFISIENSI-POMPA-HIDRAM-PARALEL-EMPAT-KATUP-ilham-Pramono/8fc876ec3df8e19d825cb74687dc7bcc196e6a6e?utm_source=direct_link
- Rajaonison, A., & Rakotondramiarana, H. T. (2020). Experimental validation of a mathematical model of the operation of a hydraulic ram pump with a Springs system. *American Journal of Applied Sciences*, 17(1), 135-140. DOI: <https://doi.org/10.3844/ajassp.2020.135.140>
- Rennie, L. C., & Bunt, E. A. (1990). The automatic hydraulic ram—experimental results. *Proceedings of the Institution of Mechanical Engineers, Part A: Journal of Power and Energy*, 204(1), 23-31.

- Rosenberg, D. M., Bodaly, R. A., Usher, P. J. (1995). Environmental and social impacts of large scale hydro- electric development: Who is listening? *Global Environmental Change*, 5(2), 127-148.
- Schiller, E. J., & Kahangire, P. (1984). Analysis and computarized model of the automatic hydraulic ram pump. *Canadian Journal of Civil Engineering*, 11(4), 743-750. DOI: <https://doi.org/10.1139/l84-093>
- Silver, M. (1977). *Use of hydraulic rams in Nepal: A guide to manufacturing and installation*. Edition of book: UNICEF. Recovered from <https://www.ircwash.org/sites/default/files/232.5-77US.pdf>
- Sobieski, W., Lipin, S., & Grygo, D. (2020). *An analysis of the conditions during the autonomous start-up of a water ram*. DOI: <https://doi.org/10.1007/s12046-020-1272-0>
- Sobieski, W., Grygo, D., & Lipiński, S. (2016). Measurement and analysis of the water hammer in ram pump. *Sadhana*, 41(11), 1333-1347.
- Sobieski, W., & Grygo, D. (2019). Fluid flow in the impulse valve. *Technical Sciences*, 22(3), 205-118.
- Steinmetz, M., & Sundqvist, N. (2014). *Environmental impacts of small hydropower plants-a case study of Borås energi och Miljö's hydropower plants*. Gothenburg, Sweden: Chalmers University of Technology.
- Suarda, M., Kusuma, I. G. B. W., Sucipta, M., & Ghurri, A. (2020). Investigation of tilt-angled delivery valve in hydraulic ram-experiment results. *International Journal of Mechanical Engineering and Technology (IJMET)*, 11(2), 117-129.

- Sucipta, M., & Suarda, M. (2019). Investigation and analysis on the performance of hydraulic ram pump at various design its snifter valve. *IOP Conference Series: Materials Science and Engineering*, 539(1). DOI: <https://doi.org/10.1088/1757-899X/539/1/012007>
- Tacke, J. H. P. M. (1988). *Hydraulic rams a comparative investigation*. Recovered from <https://repository.tudelft.nl/islandora/object/uuid%3Aafc050d-4500-4565-9fdc-b5d8afc3064b>
- Viccione, G., Immediata, N., Cava, R., & Piantedosi, M. (2018). A preliminary laboratory investigation of a hydraulic ram pump. *Proceedings*, 2(11), 687. DOI: <https://doi.org/10.3390/proceedings2110687>
- Watt, S. (1975). *A manual on the hydraulic ram for pumping water*. Recovered from <https://api.semanticscholar.org/CorpusID:107668235>
- Young, B. W. (1998). Generic design of ram pumps. *Proceedings of the Institution of Mechanical Engineers, Part A: Journal of Power and Energy*, 212(2), 117-124. DOI: <https://doi.org/10.1243/0957650981536646>